SIMULTANEOUS DETECTION OF VANILIN AND ASCORBIC ACID ON A PLATFORM MODIFIED WITH NICKEL TETRAAMINE PTHALOCYANINE NITROGEN DOPED GRAPHENE.

By

MARINGO JULIUS TAKUDZWA

(R143011Y)

Submitted in partial fulfillment of the requirements for the degree of

Bachelor of Science Honors in Chemical Technology

Department of Chemical Technology

In the

Faculty of Science and Technology at the

Midlands State University

Gweru, Zimbabwe

Supervisors: Prof. Mambo. Moyo

Dr Munyaradzi. Shumba

Ms Murinzi

DEDICATION

This work is dedicated to God Almighty who proved to me that nothing is impossible with him

and to my parents who stood by me against all odds, during the course of this degree

ACKNOWLEDGEMENTS

ABSTRACT

An electrochemical sensor based on nickel tetraamine phthalocyanine and nitrogen doped grapheme oxide (NITAPC-NDGONS (mix)) nanoparticles was developed for the simultaneous electrocatalytic oxidation of vanillin and ascorbic acid. FTIR (Fourier Transimition Infrared), electrochemical impedance spectroscopy (EIS) and Bode plots were used in the characterization of the synthesized modifiers (NITAPC), (GONS-NITAPC) and NITAPC-NDGONS (mix)). Cyclic voltammetry, linear sweep, chronoamperometry and differential pulse voltammetry were used to assess the electrocatalytic efficiency towards oxidation of vanillin and ascorbic acid. The surface area of the modified electrode was 0.173 cm^2 and the surface coverage was 7.60 x 10^{-13} mol cm^2. The catalytic rate constant of ascorbic acid was 1.59 x 10^8 M^{-1} s^{-1} and for vanillin it was 1.28 x 10^8 M^{-1} S^{-1} . The apparent electron transfer rate constant was 2.05 x 10^{-2} cm s^{-1} .The adsorption equilibrium constant for ascorbic acid was 6.4 x 10^2 M^{-1} and for vanillin was 8.05 x 10^2 M^{-1} . Gibbs free energy for ascorbic acid was -16.01 kJ and for vanillin was -16.57 kJ. The limit of detection was 8.6 x 10^{-8} M and the limit of quantification was 2.6 x 10^{-7} M for ascorbic acid and Limit of detection (LOD) was 2.58 x10^{-8} M and Limit of quantification (LOQ) was 6.8 x 10^{-8} M for vanillin. Interference studies were done and the electrode displayed the ability to detect both vanillin and ascorbic acid in the presence of citric acid. The electrode displayed good reproducibility.

APPROVAL

This dissertation entitled "Simultaneous detection of vanillin and ascorbic acid on a platform modified with Nickel tetraamine phthalocyanine nitrogen doped graphene oxide" by Julius .T. Maringo meets the regulations governing the award of the Hons degree of Chemical Technology of Midlands State University, and is approved for its contribution to knowledge and literal presentation.

Supervisor…………………………..

Date……………………

DECLARATION

I Maringo Julius.T , hereby declare that I am the sole author of this dissertation. I authorize Midlands State University to lend this dissertation to other institutions or individuals for the purpose of scholarly research.

Signature …………………………………

Date ……………………………………….

Table of contents

List of figures

l

List of tables

LIST OF ABBREVIATIONS

EIS - Electrochemical impedance spectroscopy

CV - Cyclic Voltammetry

DPV - Differential pulse voltammetry

LSV- Linear sweep voltammetry

CA- Chronoamperometry

AA - Ascorbic acid

GONS - Graphene oxide nanosheets

NDGONS - Nitrogen doped graphene oxide nanosheets

NITAPC- Nickel tetraamine phthalocyanine

FTIR- Fourier Transfer Infrared

UV-Vis- Ultraviolet visible spectroscopy

GCE- Glassy carbon electrode

LOD- Limit of detection

LOQ- Limit of quantification

MPCs- Metallated phthalocyanines

DMF- Dimethyl formaldehyde

SEM- Scanning Electron Microscopy

GC- Gas chromatography

HPLC- High Performance Liquid Chromatography

CHAPTER ONE

1.0 Introduction

The chapter highlights the background of the research and the various methods that were used for the electrochemical detection of vanillin and ascorbic acid. It also contains the objectives problem statement and the justification of this particular study.

1.1 Background

Vanillin is the primary chemical component of vanilla bean (fig 1.1). It is a phenolic aldehyde and organic compound with the molecular formula $C_8H_8O_3$. Its functional groups include aldehyde, ether and phenol [1].Vanillin is also called 4-hydroxy-3-methoxybenzaldehyde, para-vanillin, vanillic aldehyde,4-hydroxy-m-anisaldehyde,aldehyde,3-methoxy-4-hydroxybenzaldehyde and hydroxy-4-methoxy-3-benzaldehyde. Vanillin was first synthesized from eugenol found in oil of clove and afterward synthesized from lignin containing sulfite liquor, a by -product of wood pulp processing in paper manufacture. Vanillin (4-hydroxy - 3methoxybenzaldehyde) has a pleasant smell and is used as a flavoring additive for beverages ,cooking and as an additive for candles and incense[1]. Excessive ingestion of Vanillin can cause headaches, nausea and vomiting, and can affect potential damage to liver and kidney. Hence, it is important and necessary to detect and control the content of vanillin in food products [2].

Ascorbic acid (AA) is a critical vitamin dispersed throughout the diet of both humans and animals. In plant cells, it exists in its free form, and at the same time, it is usually bound to proteins such as ascorbigen [3]. Ascorbic acid has got a molecular formula of $C_6H_8O_6$, molar mass of 176.12g/mol .It is used in large scale as an antioxidant in food, animal feed, beverages, pharmaceutical formulations and cosmetic applications. It is also important in helping to produce

collagen, a protein needed in the development and maintenance of bones, cartilage, joint linings, skin, teeth, gums and blood vessels [4]. Ascorbic acid is a dibasic acid with an enediol group built into a five membered heterocyclic lactone ring (Fig 1.1). The chemical and physical properties of ascorbic acid are related to its structure. Ascorbic acid is a strong reducing agent and readily oxidizes reversibly to dehydroascorbic acid [5].
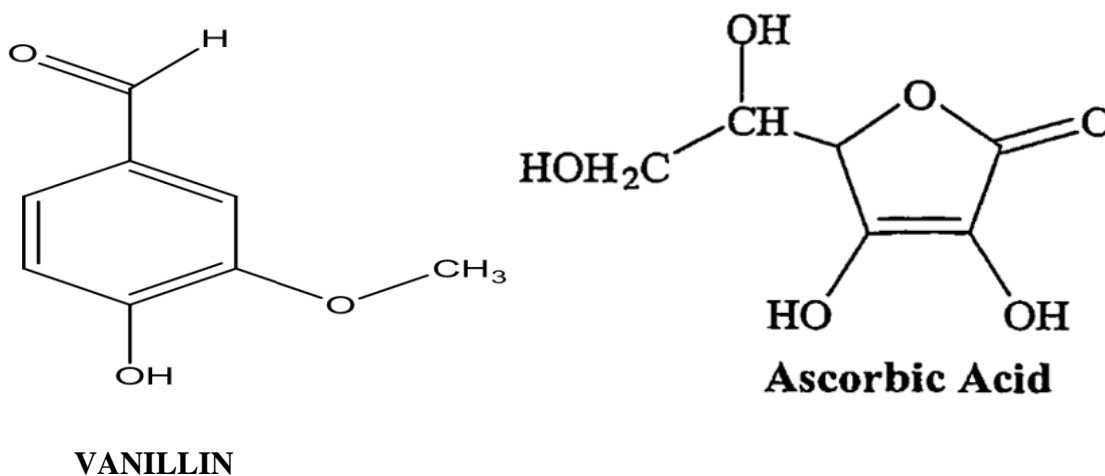
VANILLIN

Fig 1.1: Chemical structure of vanillin and ascorbic acid.
Several methods have been described in literature regarding detection of vanillin and ascorbic acid using conventional or novel techniques .Such techniques include spectrophotometry, gas chromatography coupled with mass-spectrometry (GC-MS), high performance liquid chromatography (HPLC), electrophoresis. However, these methods are more expensive and usually require sample pre- treatment, generating a great amount of residue in comparison with other analytical methods. Many analytical techniques including sensors and biosensors have been suggested for the detection of ascorbic acid in very varied types of samples. Other methods such as high performance liquid chromatography and capillary electrophoresis [4], which are based on the most commonly employed physio-chemical methods have been used for identification of AA

However on the other hand, electrochemical techniques have been proved to be more reliable and cost effective for quality control. Electrochemical methods, offer good advantages in terms of simplicity, direct use in point of care assay and portability. However, electrochemical detection of vanillin and AA at conventional bare electrodes suffers from draw backs such as high over potential and electrode fouling. These limitations can be overcomed by employing chemically modified electrodes such as nafion/lead –ruthenium oxide pyrochlore, pre-anodized nontronite coated screen printed electrodes [9], electrochemically activated multi-walled carbon nanotubes MWCNT) paste electrodes, and nickel nanoparticles.

1.2 Aim of the study

To assess the efficiency of the modified glassy carbon electrode using electrochemical detection of vanillin and ascorbic acid.

1.3 Objectives

- ➤ To synthesize nickel (II) tetra amine phthalocyanines (NiTAPc), nitrogen doped graphene (N-GO) and nitrogen doped graphene nickel (II) tetra amine phthalocyanines

- ➤ To characterize the electrode modifiers using FTIR, TEM, SEM, XRD, cyclic voltammetry and electrochemical impedance spectroscopy.

- ➤ To optimize pH for the analysis of AA and vanillin on the modified electrodes.

- ➤ To establish the reaction kinetics during electro-catalytic oxidation by CV, LSV, and Chronoamperometry (CA).

- ➤ To determine the limit of detection of vanillin and AA in buffer solution by using DPV and chronoamperometry.

- ➤ To study the effect of interferences in the presence of AA and vanillin on the modified glassy carbon electrode.

3

➢ To perform repeatability, reproducibility and stability studies of the developed electrode towards oxidation of AA and vanillin in buffer solution.

1.4 Problem statement

The presence of ascorbic acid, vanillin and their metabolites in the environment have adverse effects on environment due to the eco-toxicity potential and their exposure could also be very harmful to human health. Furthermore, AA resulted to affect also antimicrobial and natural killer cell activities, lymphocyte proliferation, chemotaxis and delayed-type hypersensitivity[6].This has resulted in the interest of the development of suitable method of analysis that is cheaper and easier to use in identifying and quantifying ascorbic acid and vanillin .The current conventional methods that are used to monitor vanillin are high performance liquid chromatography, ion chromatography, gas chromatography, paper chromatography and thin layer chromatography .However, these methods have limitations in that they are very expensive, time consuming, laboratory borne, they need a lot of skill in the operation and sometimes suffer from low detection limit. Furthermore, a large amount of sample volume and solvent are needed in separation and extraction procedure. HPLC is currently used as a clinical detection method, but is limited to a small number of laboratories due to its requirement of a highly technically skilled operator (Vogesser and Seger 2008). Due to these constraints, HPLC is far from widespread clinical application [7]. Apparently there is a need to overcome all these challenges. Consequently a cheaper, faster, easier to use, low power consuming, miniaturizable, user friendly and on site analytical device suitable to compliment or substitute for these classical methods is developed. This is done in form of nickel tetra amine phthalocyanine nitrogen doped graphene nanocomposite based electrochemical sensor for the detection and quantitative determination of both vanillin and AA .

1.5 Justification

Due to the above mentioned health problems and instrumental problems associated with both AA and vanillin there is a need to design convenient tools for the electro analysis of these compounds in food and pharmaceutical waste waters. Electrochemical techniques particularly cyclic voltammetry (CV), chronoamperometry and square wave voltammetry (SWV) are employed as alternative methods for the detection and electrochemical characterization of vanillin and AA. Characteristics of electrochemical sensing systems include high sensitivity and selectivity, a wide linear range, minimal space, power requirements and low cost instrumentation. Therefore in the present study MPcs and nitrogen doped graphene are used as they have good electron transfer properties, chemically linking them together could produce very good electron transfer mediators for electro catalysis. Also, MPcs carrying electro active metal like Ni have excellent redox properties and if chemically coupled to nitrogen doped graphene; very efficient electrochemical sensors could be produced. Nickel tetra amine phthalocyanine were used in this study as they have good electro catalytic properties due to their high electron density, easy to synthesize and also the presence of the peripheral groups on ring that can be fine-tuned in order to increase its catalytic properties. Nitrogen doped graphene were also used in this study because of good environmental stability, ease of synthesis, low cost, high electrical properties (due to their delocalized π-π conjugated systems), mechanical flexibility and the substitution of carbon atoms in the honeycomb lattice by heteroatoms ,such as nitrogen, would disrupt sp^2 hybridization of carbon atoms ,thus effectively tailoring the electronic properties .Nitrogen doping can tune graphene from being a p type to an n-type semiconductor. As a two-dimensional (2D) carbon material, graphene exhibits excellent properties which provide low-cost manufacture, high mechanical strength, good conductivity and high surface area .Graphene also has shown excellent electron transfer properties towards lead, catechol and hydroquinone [8]. It

has been found that the Fermi potential can be changed based on nitrogen doping, thus greatly improving the electron transfer efficiency of graphene and resulting in desirable properties for electro analysis of vanillin and AA. The modifiers were combined together in order to reduce the over potential of the bare glassy carbon electrode and also to increase sensitivity towards the detection of AA and vanillin.

CHAPTER TWO

2.0 Literature review

This chapter gives an outline of ascorbic acid, vanillin, nickel tetra-amine phthalocyanines and all the theory of electrochemical analysis.

2.1 Ascorbic acid

Ascorbic acid, the reduced form of vitamin C, is an essential metabolite for a variety of organisms. It is present in multiple fruits and vegetables and is also synthesized from glucose in the liver of many mammalian species, allowing the maintenance of physiological levels [9]. Ascorbic acid is widely distributed in nature, mostly rich in fresh fruits and leafy vegetables such as guava, mango, papaya, cabbage, mustard leaves and spinach (Tee *etal.,* 1997). Animal sources of this vitamin such as meat, fish, poultry, eggs and dairy products contain smaller amounts and are not significant sources [11].

The side effects of normal vitamin C intake are very minor, if non-existent, due to the fact that it is water soluble and quickly excreted. There have been some reports of negative effects in larger doses, and to help prevent that, the USDA set the upper tolerable limit (UL) for vitamin C at 2 g. Gastrointestinal distress and diarrhea are the most common side effects, which have been shown in single oral doses of 5-10 g or greater than 2 g daily, with symptoms disappearing within 1-2 weeks. There has been evidence to suggest a few more severe side effects with high-dose vitamin C. The most note-worthy is the production of calcium oxalate stones in patients with renal issues (though some healthy individuals can also produce excessive oxalate at doses greater than 1 g daily). This is because vitamin C converts to oxalate during the elimination process, which can cause formation of stones at high [16].

Ascorbic acid with antidepressants significantly decreased the total Hamilton depression rating scale [10]. Several symptoms of ascorbic acid deficiency have been recognized including follicular hyperkeratosis, swollen and inflamed gums, loosening of teeth, dryness of the mouth and eyes, loss of hair and dry itchy skin. These symptoms reflect the role of ascorbic acid in the maintenance of collagen and blood vessel integrity [11]. The recently released Recommended dietary allowance of vitamin C for women is 75 mg daily [12]. The electro catalytic oxidation of ascorbic acid occurs at slightly low pH between 6 -7. Its oxidation is also affected by the choice of the supporting electrolyte employed, which can be PBS or Na_2SO_4. The process of oxidation of ascorbic acid involves the release of two electrons (e-) and along the release of electrons ascorbic acid also releases two protons and a new stable molecule dehydroascorbic acid (Fig 2.0). The reaction is an equilibrium reaction, which means it can go back and forth. However dehydroascorbic acid is very unstable and can further react.
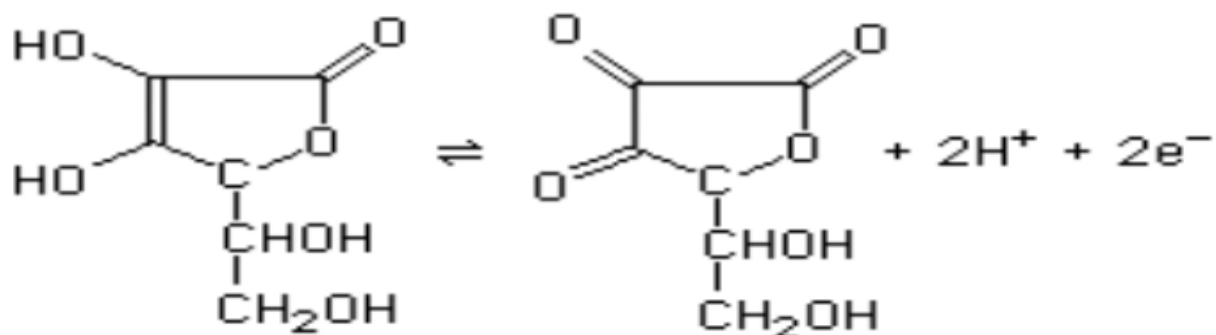
Fig 2.1: Oxidation of ascorbic acid

2.2 Vanillin
Vanillin is a white crystalline material melting at about 81°C. The purity is generally above 99.0% w/w on dried basis ,vanillin has a characteristic pleasant smell and taste of vanilla which

is reason for its widespread use[13] . Vanillin (4-hydroxy-3-methoxybenzaldehyde) is one of the world's flavor extracts obtained primarily from Vanillia planifolia, a specie of tropical climbing orchid native to Mexico or Central America [14]. Vanillin is soluble in water and solubility increases with increasing temperature. At $25^{\circ}C$, the solubility is 10 g/l. Log P_{ow} value ranges from 1.21 to 1.35 [13] .

Vanillin also used as inhibition of the oxidation of human low density lipoproteins, which leading to lower rates of cardiac disease mortality [2], and used as an anti-sickling effect in sickle cell anemia sufferers. So, controlling the quality of vanillin is of great importance[14] .It is unclear if synthetic biology vanillin is safe to eat, or what impacts if the synthetic organisms may have upon were interact with natural organisms or ecosystems. We do not have adequate regulatory agencies or sufficient independent data to determine this. Without precautionary testing and regulations that are specific to synthetic biology and which recognize it is as a unique and complex technology, we may not find emergent health threats until it is too late [15].

2.3 Graphene oxide

Graphene oxide is an oxygenated derivative of grapheme and it contains many functional groups on its surface including epoxy groups, carboxyl groups and hydroxyl groups. Graphene has excellent electrical, mechanical and thermal properties [47].Graphite oxide sheets ,now called grapheme oxide (GO) is the product of chemical exfoliation of graphite with strong oxidizing agents such as $KMnO_4$ in concentrated sulphuric acid. The oxidation of graphite breaks up the extended two-dimensional (2D) Л-conjugation of the stacked grapheme sheets into nano-scale graphitic sp^2 domains surrounded by disordered ,highly oxidized sp^3 domains as well as defects of carbon vacancies. The severe functionalization of the conjugated network renders the GO

sheets insulating ,however conductivity may be partially restored conveniently by thermal or chemical treatment ,producing chemically modified grapheme sheets[46] as shown in (Fig 2.2) .The interruption of the lattice is reflected by an increase in interlayer spacing from 0.335 nm for graphite to more than 0.625 nm for GO.
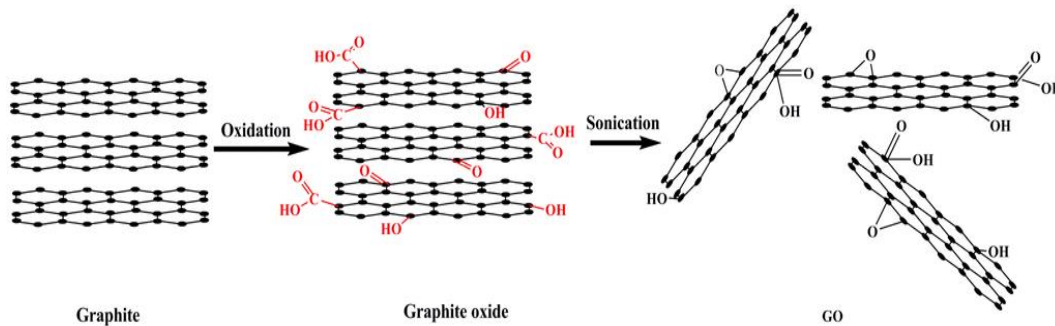
Fig 2.2: Formation of GO sheets

2.4 Nitrogen doped graphene oxide

Graphene oxide has a carbon to oxygen atomic ratio (C/O) of around 2 [46] and a zero band gap semiconductor, which limits application potential due to its chemical inertness. It is known to exhibits high surface areas (theoretical specific surface area of 2620 m^2 g^{-1}). Chemical modification of GO converts it to an electrically conducting state by increasing its C/O above 6. Chemical doping with heteroatoms such as nitrogen or boron of graphene has become very necessary since it creates a band gap and this is useful for various applications.

It provides pathways for efficient electron transfer processes since free charge carriers has increased in the graphene frame work, transforming graphene into a p or n type semiconductor. Nitrogen doped graphene were also used in this study because of good environmental stability, ease of synthesis, low cost, high electrical properties (due to their delocalized π-π conjugated systems), mechanical flexibility and the substitution of carbon atoms in the honeycomb lattice by heteroatoms, such as nitrogen, would disrupt sp^2 hybridization of carbon atoms, thus

effectively tailoring the electronic properties .It has been found that the Fermi potential can be changed based on nitrogen doping ,thus greatly improving the electron transfer efficiency of graphene and resulting in desirable properties for electro catalysis. . The nitrogen doping of graphene has been done by thermal annealing in the presence of ammonia and the nitrogen atom in the graphene frame work can exist in graphitic, pyridinic or pyrrolic forms as shown in (Fig 2.3)
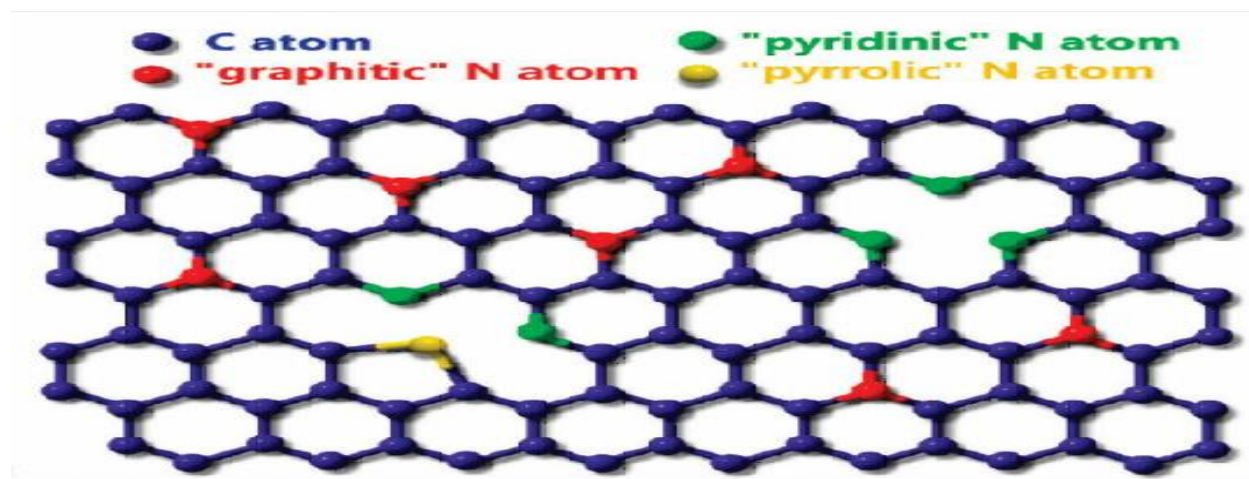
Fig 2.3: Structure of Nitrogen doped graphene oxide

2.5 Phthalocyanines

Pcs are highly colored, planar 18 π-electron aromatic ring systems similar to porphyrins. A phthalocyanine containing one or two metal ions is called a metal phthalocyanine (M-Pc). The central cavity of phthalocyanines is known to be capable of accommodating 63 different elemental ions, including hydrogen (metal-free phthalocyanine, H_2-Pc) [47] .Pcs are composed of four pyrrole units linked by four aza (—N=C—) groups at the α-carbon of pyrrole unit and they have four aza bridges and four phenylene rings as shown in (Fig 2.4) .Nickel tetraamine phthalocyanine is synthesized by reacting 4-nitrophthalic acid ,nickel (II) sulphatepentahydrate, ammonium chloride , ammonium molybdate and urea to form crude NiTNPc which will be

washed with with ethanol to remove nitrobenzene and then boiled in 60ml of 1M HCL to give a

dark blue dye/pigment.
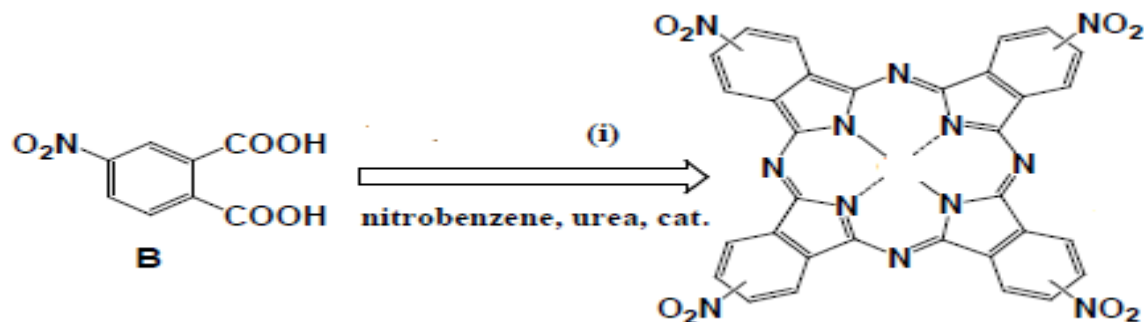
Fig 2.4; Formation of phthalocyanines (NITNPc)

The crude NITNPc is treated with sodium sulphidenona hydrate in water and centrifuged to give

a dark greenish product of NiTAPc [48] as shown in (Fig 2.5).
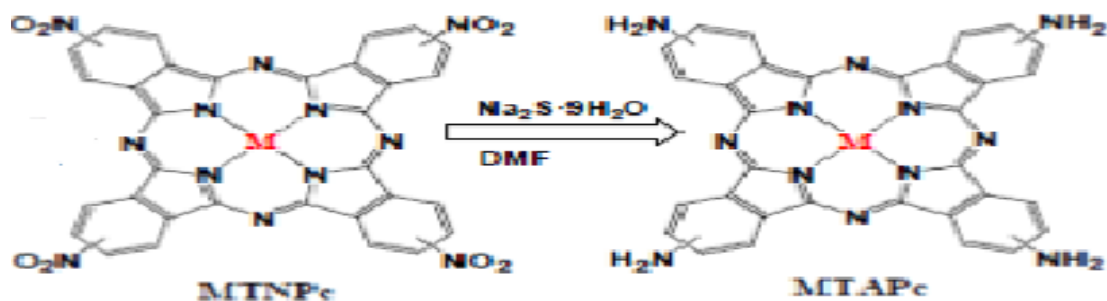
Fig 2.5 Formation of NITAPC

A Pc molecule consists of a central cavity that can accommodate different metal ions.

Introduction of metal cations (e.g. Fe^{2+}, Zn^{2+}, Co^{2+} etc.) into the central cavity of Pc molecule

influences its physical properties greatly. According to X-ray analysis, the central metal atom

with a +2 oxidation state is bonded to two nitrogen atoms by covalent bonds and to the other two

nitrogen atoms by coordinate covalent bonds.

2.6 Application of metal- phthalocyanine (M-Pcs)

As a result of their high electron transfer abilities, MPcs have been utilized in many fields such as molecular electronics, optoelectronics, photonics, etc. The functions of MPcs are almost universally based on electron transfer reactions because of the 18 pi- electron conjugated ring system found in their molecular structure [47] .Typical function of phthalocyanine derivatives: photosensitization, photovoltaic light absorption, photoconductivity, conductivity, electronic sensors, solar cells, photodynamic therapy, optical disks, synthetic metals, catalysts, optoelectronics, liquid crystals. Further, particular derivatives are known to have potential as second-generation photosensitizers for photodynamic therapy (PDT) of cancer [50] because they show strong absorption of the far-red light between the wavelengths of 600 and 850 nm, which has greater tissue penetration properties [51], and satisfactory photosensitization of singlet oxygen [49].
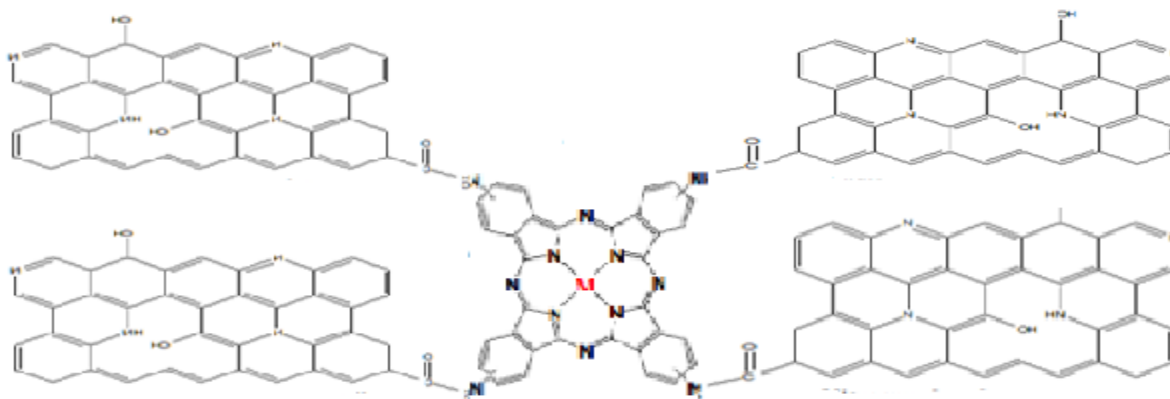
Fig 2.6; Structure of NiTAPc-NGO

2.7 Electrode modification techniques

The structure of the interface electrode/electrolyte, i.e. where the electrochemical reaction proceeds, is of decisive importance for an electrode reaction. If one is able to control the physical

and chemical properties of this interface, then reactivity, selectivity, etc., can be obtained. One of the main purposes of surface modification is the introduction of specific catalytic centre's at an electron-conducting material [17]. We also discover the two major reasons for wanting to attach molecules to electrode surfaces. As explained by Lane and Hubbard, one objective is to obtain fundamental information about the mechanism of electron transfer at electrode surfaces. The second objective, as expressed by Miller at al. and Elliott and Muffay, is to impart to the electrode surface some chemical specificity not available at the unmodified electrode [18].

Electrodes encounter specific phenomena that reduce their applicability to analytical and synthetic schemes, which include electrode fouling by unwanted precipitation or adsorption processes. These phenomena often can be controlled by manipulating the chemical nature of the electrode surface. When an electrode, such as a piece of platinum or carbon is dipped into a solution, its surface becomes covered with a layer of water molecules. Sometimes species present in the solution that have been purposely added or are present as impurities will also attach to the electrode surface [16]. These particles may cause the observed current to be smaller because they block access to the surface of the electrode.

Modified electrodes can be prepared by several different techniques and are therefore often referred to by such names as derivatized , polymer-coated, functionalized, and electrostatically-bound electrodes[16].

Applications- important applications of chemically modified electrodes (CME) include energy conversion and storage, controlled release of drugs, electrochromic displays, corrosion protection and electro-organic synthesis [19]. CMEs has found a vast range of applications including environmental monitoring, industrial quality control, and biomedical analysis (Wang

et a l , 2000)

2.7.1 Chemical modification

Chemisorption is an adsorptive interaction between a molecule and a surface in which electron density is shared by the adsorbed molecule and the surface. Chemisorption requires direct contact between the chemisorbed molecule and the electrode surface; as a result, the highest coverage achievable is usually a monomolecular layer. Chemisorption is rarely completely irreversible. An example of chemisorption is shown in equation 2.1 where gold (Au) and alkythiol (RSH) reacts. The reaction is typically carried out by simply immersing the electrode into a dilute solution of the thiol.

Au + R-SH → -Au-S-R + 1/2 H₂   (2.1)

In most cases, the chemisorbed molecules slowly leach into the contacting solution phase during electrochemical, or other, investigations of the chemisorbed layer. For these reasons, electrode modification via chemisorption was quickly supplanted by other methods, most notably polymer-coating methods [18].

2.7.2 Covalent attachment

This chemistry has since been used to attach an enormous number of functional groups to SnO_2, RuO_2, TiO%, Pt, Au, and other electrode surfaces.

$$-M\text{-}OH$$
$$-M\text{-}OH + Cl_3\text{-}Si\text{-}CH_2CH_2\text{-}R \longrightarrow -M\text{-}O\text{-}Si\text{-}CH_2CH_2\text{-}R + 3HCl$$
$$-M\text{-}OH \qquad\qquad\qquad -M\text{-}O$$

(2.2)
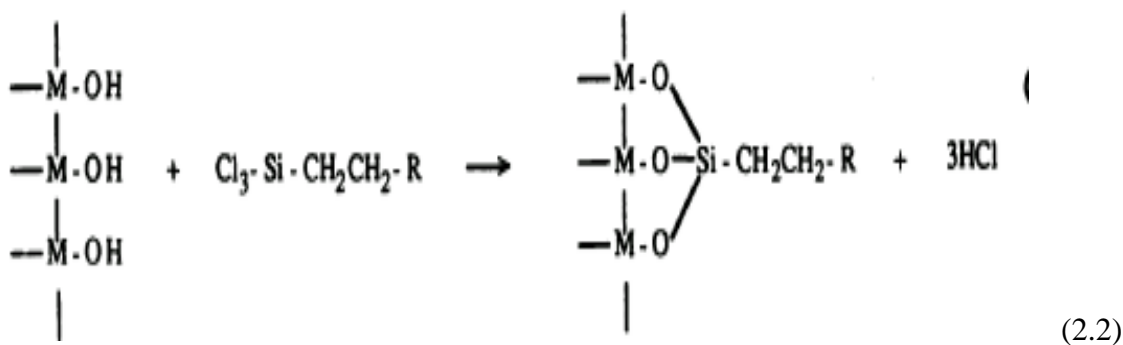
Fig 2.7: Illustration of covalent attachment

The example involves reaction of a surface hydroxyl with a hydrolytically-unstable silane. This chemistry is illustrated in equation in (Fig 2.7) where M-OH represents a hydroxyl group on an electrode surface and R on the silane is the functional group that is to be attached to the electrode surface. Equation above should be viewed as a "cartoon' version of the 'salinization" reaction because while the silane is, in principle, capable of forming three covalent bonds to the surface, it is doubtful that all three actually form [18].

2.7.3 Composite electrodes

A composite electrode as "a material consisting of at least one conducting phase with at least one insulator phase**.** Classification of disperse composites as materials in which the particles are randomly distributed by the material, such as in carbon pastes and polymer agglutinated materials, and consolidated composites in which the conductive particles occupy specific areas of the material. A polymer can replace the liquid in order to prepare a rigid composite electrode material. The main advantages are the mechanical resistance and the enlargement of the possibilities of use in non-aqueous medium [20].

2.8 Electrochemistry

Electrochemistry is the study of reactions in which charged particles (ions or electrons) cross the interface between two phases of matter, typically a metallic phase (the electrode) and conductive solution, or electrolyte. A process of this kind is known generally as an electrode process [22].

2.9 Voltammetry

A time-dependent potential is applied to an electrochemical cell, and the current flowing through the cell is measured as a function of that potential. The common characteristic of all voltammetric techniques is that they involve the application of a potential (E) to an electrode and the monitoring of the resulting current (i) flowing through the electrochemical cell. Thus, all voltammetric techniques can be described as some function of E, i, and t. They are considered active techniques (as opposed to passive techniques such as potentiometry) because the applied potential forces a change in the concentration of an electroactive species at the electrode surface by electrochemically reducing or oxidizing it [21]. Unlike potentiometric measurements, which employ only two electrodes, voltammetric measurements utilize a three electrode electrochemical cell. The use of three electrodes (working, auxiliary and reference) along with the potentiostat instrument allows accurate application of potential functions and measurement of the resultant current [24]. In all electrochemical methods, the rate of oxidation & reduction depend on:

1) Rate & means by which soluble species reach electrode surface (mass transport)

2) Kinetics of the electron transfer process at electrode surface (electrode kinetics),

which depend on:

a) Nature of the reaction
b) Nature of electrode surface
c) Temperature

2.10 Modes of mass transfer in voltammetry

Three types of mass transport are available in an electrochemical experiment:

a) **Diffusion**

 molecular motion down a concentration gradient[44]

The maximum diffusion current is given by (i_d) avg = 607 n $CD^{1/2}m^{2/3} t^{1/6}$........   (2.3)

where

$\textbf{i}_\textbf{d}$ = the average current (in micro-amperes) flowing during the life of a drop,

n = the number of equivalents per mole of the electrode reaction,

o = the diffusion coefficients of the electroactive substance in square

centimeters per second,

C = the concentration of the electroactive material in millimoles per litre,

m = the mass flow rate of mercury through the capillary in milligrams per

second,

t = the drop time in seconds.

b) **Convection**

Molecular motion imposed by bulk motion of the medium (e.g., vibrations or stirring)

c) **Migration**

 Molecular motion down an electric gradient.   In most cases migration is undesirable and can be

eliminated by adding a 100 fold excess of an inert electrolyte.

Migration is generally eliminated by the addition of a fully dissociated electrolyte, which acts as

the ionic charge carrier. Convection can also be eliminated to a certain extent by using an

unstirred solution, although it is difficult to completely eliminate natural convection (e.g., due to

vibrations and density gradients).

2.11 Cyclic voltammetry

Cyclic voltammetry is a method for investigating the electrochemical behavior of a system. Cyclic voltammetry is the most widely used technique for acquiring qualitative information about electrochemical reactions. The power of cyclic voltammetry results from its ability to rapidly provide considerable information on the thermodynamics of redox processes, on the kinetics of heterogeneous electron-transfer reactions, and on coupled chemical reactions or adsorption processes [24]. CV is a potential sweep technique. It involves sweeping the electrode potential between potential limits at a known sweep rate (also called scan rate). On reaching limit E2 the sweep is reversed to E1 to obtain a cyclic scan.

The CV scan is a plot of current verses potential and indicates the potential at which redox process occur. The potential axis is also a time axis that is related to scan rate [25] .The important parameters of a cyclic voltammogram are the magnitudes of anodic peak current (ipa), the cathodic peak current, the anodic peak potential and cathodic peak potential . From the sweep-rate dependence of the peak amplitudes, widths and potentials of the peaks observed in the voltammogram, it is possible to investigate the role of adsorption, diffusion, and coupled homogeneous chemical reaction mechanisms [26]. Equilibrium requires that the surface concentrations of O and R are maintained at the values required by the Nernst Equation [24].

2.11.1 The Nernst equation:

$$E_{cell} = E_0 - (RT/nF) \ln (c_R/c_O) \qquad (2.4)$$

Ecell is related directly to [O] and [R].

CV has become a very popular technique for electrochemical studies of new systems, and has proved as a sensitive tool for obtaining information about fairly complicated electrode reactions [27].

2.12 Electrochemical impendence spectroscopy

Electrochemical impedance is the response of an electrochemical system (cell) to an applied potential. Impedance is a measure of the ability of a circuit to resist the flow of electrical current. The term impedance refers to the frequency dependent resistance to current flow of a circuit element (resistor, capacitor, inductor, etc.) Impedance assumes an AC current of a specific frequency in Hertz (cycles/s).

Impedance: $Z_\omega = E_\omega/I_\omega$ where:

E_ω = Frequency-dependent potential

I_ω = Frequency-dependent current

The current is measured instantaneously before each potential change, and the current difference is plotted as a function of potential [28]. The Nyquist plots obtained in electrochemical impedance spectroscopy comprise of a straight line and a semi-circle. The diameter of the semicircle corresponds to the charge transfer resistance and diffusion controlled process respectively. The straight line portion represents the Warburg impedance which takes into account the frequency dependence on diffusion transportation to the electrode surface. There are several reasons to run an electrochemical impendence spectroscopy such as , EIS may be able to distinguish between two or more electrochemical reactions taking place, EIS can identify diffusion-limited reactions, e.g., diffusion through a passive film, EIS provides information on the capacitive behavior of the system, EIS can test components within an assembled device using

the device's own electrodes and EIS can provide information about the electron transfer rate of reaction. Applications of EIS include Study corrosion of metals. Study adsorption and desorption to electrode surface, study the electrochemical synthesis of materials, study the catalytic reaction kinetics ,can be used in labeling of free detection sensors and to study the ions mobility in energy storage devices such as batteries and super capacitors.

2.13 Square wave voltammetry (SWV)

Square wave voltammetric (SWV) technique is among the most sensitive means, for the direct evaluation of concentrations; it can be widely used for the trace analysis, especially on pharmaceutical compounds. Compared to other voltammetric techniques a square wave voltammetry (SWV), has a several advantages such as high speed, increased analytical sensitivity and relative insensitivity [42]. Square wave voltammetry employs scan rates up to 1 V/sec or faster, allowing much faster determinations. A symmetrical square wave is superimposed on a staircase waveform where the forward pulse of the square wave (pulse direction same as the scan direction) is coincident with the staircase step. The reverse pulse of the square wave occurs half way through the staircase step [43]. The waveform used for square wave voltammetry is shown in (Figure 2.8).
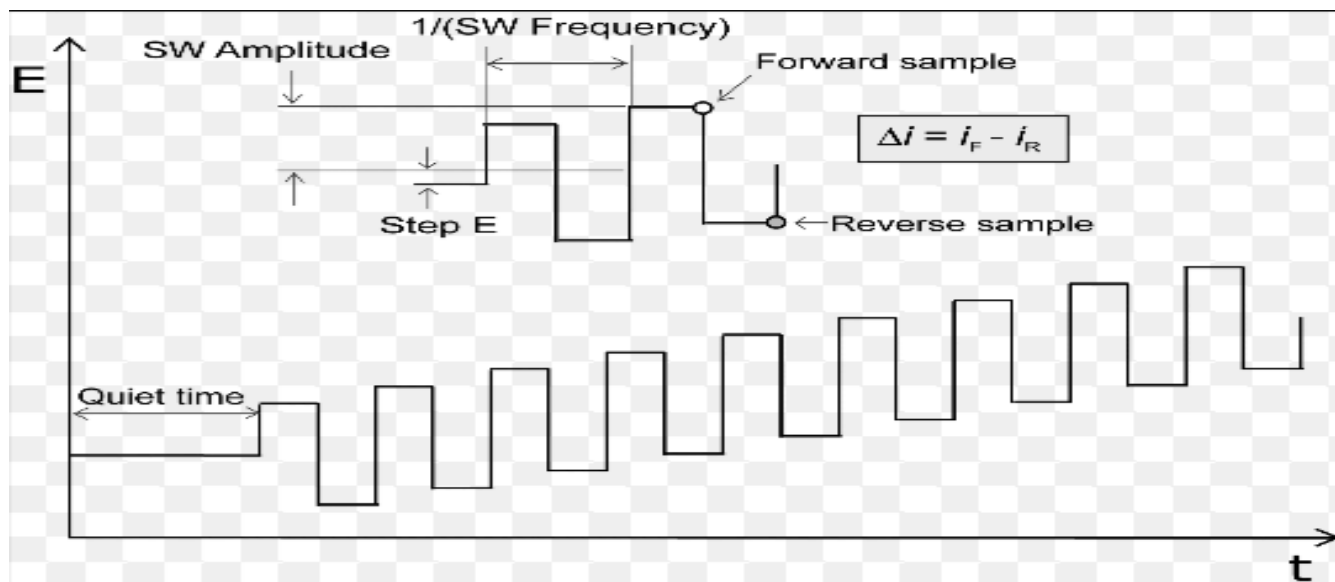
Fig 2.8: Formation of square wave

2.14 Differential pulse voltammetry (DPV)

This technique is comparable to normal pulse voltammetry in that the potential is also scanned with a series of pulses. However, it differs from NPV because each potential pulse is fixed, of small amplitude (10 to 100 mV), and is superimposed on a slowly changing base potential. Current is measured at two points for each pulse, the first point (1) just before the application of the pulse and the second (2) at the end of the pulse as shown in (Fig 2.8). These sampling points are selected to allow for the decay of the non-faradaic (charging) current. The difference between current measurements at these points for each pulse is determined and plotted against the base potential [45].

22
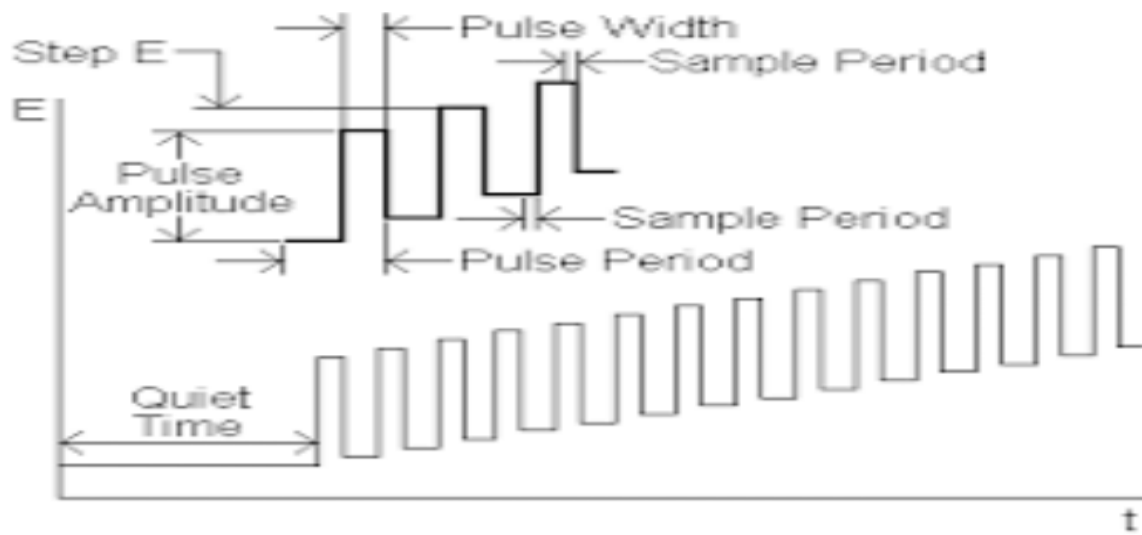
Fig 2.9: Formation of a differential pulse

CHAPTER THREE

Materials and methods

3.0 Introduction

This chapter highlights the reagents and the procedures which were applied in the study in order to address and achieve the aims and objectives. The efficiency of the NITAPC-NDGONS/GCE modified glassy carbon electrode was characterized using cyclic voltammetry and electrochemical impedance. Electro-oxidation of vanillin and ascorbic acid was studied using differential pulse voltammetry (DPV), linear voltammetry and cyclic voltammetry. The simultaneous electro-oxidation of vanillin and ascorbic acid was studied using DPV.

3.1 Reagents and chemicals

All the chemicals which were used in this study were of pure analytical grade. Potassium ferrocyanide ($[Fe(CN)_6]^{-3/-4}$) ,vanillin were obtained from Skylabs, Zimbabwe ,ascorbic acid ,nickel(ii) sulphatepentahydrate ,4- nitrophthalic acid ,ammonium chloride ,30% ammonia ,ammonium molybdate ,nitrobenzene, Graphite, potassium permanganate ($KMNO_4$), concentrated sulphuric acid, hydrogen peroxide(30%), sodium nitrite, hydrochloric acid, urea, sodium hydroxide, sodium sulphidenonahydrate, DMF. Distilled water was from Midlands State University Chemical Technology laboratories. A stock solution of potassium ferricyanide was dissolved in 1MKCl in a 500 ml volumetric flask.

3.2 Equipment

All the electrochemical experimental procedures were carried out using Auto lab Potentiostat PGSTAT 302F installed a1.10 version NOVA software employing a convectional three electrode

system. The three electrode system constituted of a bare glassy carbon electrode of 3 mm in diameter which was the working electrode, a platinum wire which was working as an auxiliary/counter electrode and Ag/AgCl (3.0 M) which was working as the reference electrode. All the experiments that were conducted in the study were carried out at room temperature conditions 25 °C. A digital analytical balance (G and G of model JJ224BC) was used for weighing. As for pH studies of the solutions, they were adjusted by a Thermo-scientific Orion Star A211 pH meter.

3.3 Synthesis of graphene oxide

Graphene oxide (GO) was synthesized by Hummers method , 2,041 g of graphite powder , 0.987 g of sodium nitrite and 44 ml of concentrated sulphuric acid was mixed together and stirred using magnetic stirrer .After 1 hour 5,987 g of $KMnO_4$ is added gradually to the solution and the temperature was maintained at less than 20°C to prevent overheating and explosion. The mixture was stirred at 35°C for 30 minutes and then 92 ml of water is slowly added. The resulting mixture is maintained at 98°C for 15 minutes then the heat is removed. An additional 280 ml of Water and 30% hydrogen peroxide (H_2O_2) is added. The final mixture was washed with HCl and deionized water respectively and dried for overnight at 60°C [65].

3.4 Synthesis of nitrogen doped graphene

A 500 mg of GO was added to 600 ml of di- ethylene glycol under ultra-sonication for 4 h to obtain a well-dispersed GO suspension. A 100 ml of ammonia solution was added and vigorously stirred for 10 min, and then it refluxed at 180 ^{0}C for 10 h. The precipitate was then isolated by vacuum filtration, washed with ethanol and deionized water, then dried at 80 ^{0}C overnight [66]. Incorporation of nitrogen was checked by characterizing with FTIR.

3.5 Synthesis of Nickel tetra nitro phthalocyanine (NiTNPc)

 4-nitrophthalic acid 1.13 g, nickel (II) sulphatepentahydrate (0.37 g), ammonium chloride (0.138) g, ammonium molybdate (0.013 g) and urea (0.138 g) were finely ground and nitrobenzene 35 ml added. The reaction mixture was heated at 185 ^{0}C for 4 hours. Crude NiTNPc was washed with ethanol to remove nitrobenzene and then boiled in 60 ml of 1 M HCl (saturated with sodium chloride) for 5 minutes before filtering .The resulting solid was heated in 60 ml of 1 M NaOH at 90 ^{0}C until ammonia evolution ceased which took approximately 6 hours. After filtering the dark blue solid was alternatively treated with 1 M HCl and 1 M NaOH two times and finally washed with deionized water to afford NiTNPc.

3.6 Synthesis of Nickel tetra amine phthalocyanine

NiTNPc (0.253 g) and sodium sulphidenonahydrate (1.265 g) was placed in 6.5 ml of water. The mixture was stirred at 50 ^{0}C for 5 hours and then centrifuged to collect the crude NiTAPc from reaction mixture .The dark greenish crude product was treated with HCl (1 M) followed by aqeous. NaOH (1 M) for an hour each before centrifugation. The solid was washed with deionized water and centrifuged to give NiTAPc.

3.7 Synthesis of NITAPC-NDGONS (MIX)

A mass of 2 g of NiTAPc was combined with 5 mg of nitrogen doped graphene in 25 ml of DMF with stirring and heated at 70 ^{0}C for 96 hours. After cooling the mixture was centrifuged and the resultant solid NiTAPc-NGO was washed several times with distilled water and ethanol. Then resultant solid was dried and stored in a desiccator to carry out further studies.

3.8 Electrode modification

A bare GCE was polished with alumina slurry powder (100 µm) on a Buehler-felt pad. It was then rinsed ultrasonically with deionized water and ethanol in the ratio 1:1 and dried at room temperature before use. 1 mg of each modifier was dispersed in 1 ml of DMF and ultra-sonicated for 30 min. The drop and dry method was used for electrode modification where 5 µl of graphene oxide and nitrogen doped graphene suspension was casted on the surface of GCE and dried in an oven at 60 ^{0}C. Prior to use, the modified electrode was cooled to room temperature.

3.9.0 Cyclic voltammetry

3.9.1 Characterization of the modified electrodes in 1 mM [Fe (CN)$_6$]$^{-3/-4}$

Cyclic voltammetry was used for the investigation of electrochemical behavior of the bare GCE, graphene oxide (GO-GCE), nitrogen doped graphene (NDGO-GCE) ,(NITAPC-NDGONS mix-GCE) electrodes in 1 mM [Fe(CN)$_6$]$^{-3/-4}$ solution at a scan rate of 0.1 V/s from -0.2 to 0.6 V.

3.6.2 Electrochemical Impedance Spectroscopy.

Electrochemical impedance spectroscopy was carried out in 1 mM [Fe (CN)$_6$]$^{-3/-4}$ solution for BGCE, GO-GCE , NDGO-GCE, (NITAPC-NDGONS -GCE), at a scan rate of 0.1 mV/s at 0.4 V, so that the electron transfer resistance of the electrode and the structural difference of the modifiers on the surface of electrode during catalysis will be noted in correspondence to results obtained in cyclic voltammetry.

3.6.3 Effect of scan rate in 1 mM [Fe(CN)$_6$]$^{-3/-4}$

Scan rate studies were done in 1 mM [Fe(CN)$_6$]$^{-3/-4}$ solution by using nitrogen doped graphene (NGO) electrode in order to determine the surface area of the modified electrode. The scan rates which were applied were 50 m V/s to 400 m V/s at a potential range of -0.2 to 0.6 V.

3.7.0 Optimization

3.7.1 Effect of pH

Two solutions of 1 mM vanillin and ascorbic acid solution in phosphate buffer was prepared and filled in six different 100 ml volumetric flasks. Each solution in 100 ml volumetric flask was adjusted its pH using 0.1 M HCl solution for acidic pH and 0.1 M NaOH solution for basic pH from pH 3 to 8. Scan rate of 0.1 V/s at a potential range of -0.2 to 0.8 V on NGO-NITAPC/GCE was done.

3.7.2 Scan rate studies in pH 7 phosphate buffer solution

The scan rate studies were performed using cyclic voltammetry and it was carried out in pH 7 phosphate buffer solution by using NGO/GCE and NGO-NITAPC/GCE modified electrode. The study was done to determine the effective surface coverage of the modified NGO/GCE. The scan rates which were applied were 50 m V/s to 400 m V/sat a potential range of 0 to 1.0 V.

3.7.3 Electrocatalytic detection of 1 mM vanillin and ascorbic acid

The electrochemical behavior of vanillin and ascorbic acid was studied using cyclic voltammetry on bare GCE, GO-GCE, NDGONS-GCE and NITAPC-NDGONS-GCE electrodes in 0.1 M phosphate buffer at pH 7 as the supporting electrolyte at 0.1 V/s.

3.8 Order of reaction

The order of reaction of NDGONS-NITAPC-GCE was studied using linear scan voltammetry in different concentrations of vanillin and ascorbic acid of 5 mM ,10 mM ,15 mM, 20 mM ,25 mM and 30 mM at 0.1 V/s scan rate and potential of 0V to 1.0 V.

3.9 Effect of interference

To the vanillin(150 μM) and ascorbic acid (120 μM) solutions was added to 5 ml volumes of 100 μM citric acid and from 0 to1.5 V potential and amplitude of 0.05 V using DPV.

3.10 Stability studies

As for the stability studies of the produced sensor, cyclic voltammetry technique was employed. The assay reproducibility of the sensor was investigated through repetitive measurements of the 500 μM vanillin sample in 0.1 M phosphate buffer solution at pH 7 at a potential of 0.6 to 1.6 V.

3.11 Sensitivity/ Limit of detection (LOD) and limit of quantification (LOQ).

Differential pulse voltammograms of vanillin solution for individual determination at different concentrations were obtained from a range of 0.2 to 1.4 μM at potential of 0 to 0.9 V, scan rate of 0.01 V/s and an amplitude pulse 0.05 V as indicated in table 3.1. Then for the individual oxidation of ascorbic acid different concentrations ranging from 0 to 1.4 μM at a potential of 0 to 0.8 V, scan rate 0.01 V/s, modulation time 0.5 s and amplitude of 0.05 V was used for analysis. As for simultaneous determination, 0.5 to 25 μM of vanillin concentrations and ascorbic acid at constant 100 μM solution was prepared in pH 7 phosphate buffer solution. Then 80 to 260 μM concentrations of vanillin and ascorbic acid solution at constant 10 μM was prepared in pH 7 phosphate buffer solution at a potential of 0.4 to 1.2 V scan rate 0.01 V/s, modulation time 0.05 s and an amplitude 0.05 V. Then 10 to 90 μM of both vanillin and ascorbic acid solution were prepared in pH 7 phosphate buffer solution at a potential of 0.4 to 1.2 V and run at scan rate 0.01 V/s, modulation time 0.5 s and an amplitude 0.05 V.

Table 3.1: Parameters for DPV

Initial potential (V)	0.400
End potential (V)	1.200
Step potential (V)	0.00500
Modulation amplitude (V)	0.05
Interval time	0.5
Scan rate V/s	0.01

3.12 Chronoamperometry

Catalytic rate constant were performed using chronoamperometry. The studies were performed by preparing working standard solutions of 20 µM, 40 µM, 60 µM and 80 µM form 1 mM stock solution of vanillin and ascorbic acid at pH 7 phosphate buffer solution .The working standard solution were prepared in 50 ml volumetric flask and diluted to the mark with pH 7 phosphate buffer solution. The prepared working standard solutions were filled in the electrochemical cell respectively and the behavior was observed on grapheme oxide GO, nitrogen doped graphene oxide (NGO) and nickel tetramine phthalocyanine nitrogen doped graphene (NITAPC-NGO) Catalytic rate constant was obtained by plotting graph of slope against $\sqrt{}$ [Vanillin] and slope against$\sqrt{}$ [ascorbic acid]. The gradient of the slope is equivalent to πk which gives the catalytic rate constant. Parameters used in chronoamperometry as shown in table 3.2

Table 3.2 Parameters for Chronoamperometry for Catalytic rate constant studies

Set potential	(V)	0.000
Set potential	(V)	0.800
Set potential	(V)	0.800
Duration	(s)	5
Interval time	(s)	0.01

3.13 Preparation of vanilla biscuits for real sample analysis.

Commercial food biscuits were purchased from a local market, containing vanillin also containing sugar, corn starch, grinded almonds, almond aroma, vanillin, colorings agents (Beta carotenes). First of all, the solid biscuits samples were ground in a mortar with a pestle. Then, about 0.5 g of this powder, 10 ml of absolute ethanol were place into a tube and shaked by a laboratory shaker for 1 h. After centrifugation at 3000 rpm for 10 min, the clear part of the solution in the tube was used for analysis [70].

3.14 Preparation of orange fruit juice for real sample application analysis.

Orange juice were bought from Senga shops (Gweru, Zimbabwe) and freshly prepared fruit juices were obtained by fruit pressing. The fruit samples were first washed with water; the juice from the fruit was squeezed out, and filtered. Then, the obtained juice was centrifuged until a clear sample was obtained, which was subsequently analyzed. The ascorbic acid content in the fruit juice samples were determined by measuring the peak current from the calibration curves in which the Background current was subtracted and calculated using the volume measured [69].

CHAPTER FOUR

4.0 Introduction

This chapter presents results and discussion obtained experimentally. Peaks appearing in the FTIR spectrum were assigned to various functional groups. Electrochemical studies were carried out using cyclic voltammetry(CV) with bare GCE, GONS-GCE ,NDGONS-GCE and NITAPC-NDGONS electrodes in 1 mM $[Fe(CN)_6]^{-3/-4}$. Chronoamperometry, linear sweep voltammetry (LSV), differential pulse voltammetry (DPV) and electrical impedance spectroscopy (EIS) were also employed in this particular study.

F_{ig} 4.1: TEM images of a) GONS and b) NITAPC-NDGONS.
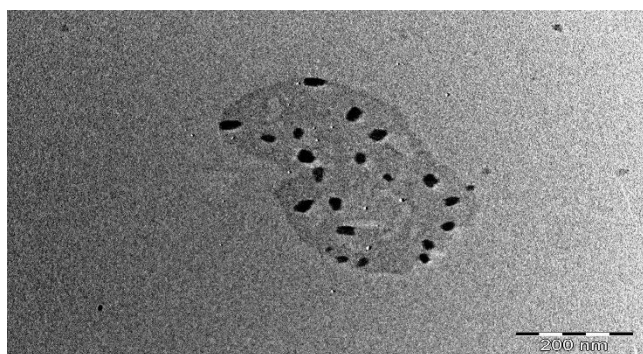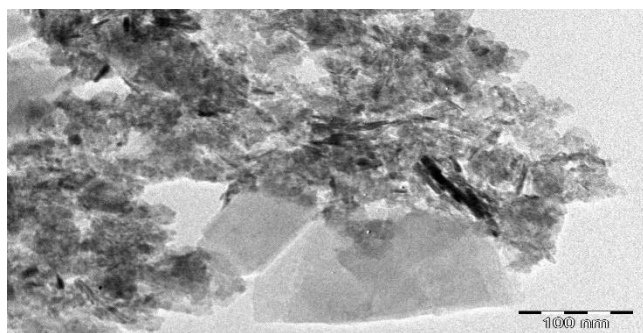
4.1.4 TEM images for GO and NITAPC-NGO (mix)

Fig 4.4 show dumb-bell shapes, with the NITAPC on both sides of the nanosheets, showing that

the carboxylic acid groups to which the amino groups are attached are on the terminal ends. The

nanoshetes are in the middle of the phthalocyanine aggregates. The lack of continuity in the

nature of NITAPC-NGO-linked nanosheets, relative to the NDGONS and the mix shows that

the nanorods. The different sizes observed in Fig 4.4 could be due to aggregation of MPc or

linking of more than one NITAPc unit to each end of the nitrogen doped graphene oxide

nanosheets.

4.1.0 Characterization

4.1.1 Fourier Transfer Infrared Spectroscopy.

Fig 4.1 shows the obtained peaks of GO and NGO. The spectrum of GO shows peaks at the

presence of different types of oxygen functionalities in graphene oxide were confirmed at broad

and wide peak at 3500 cm^{-1} can be attributed to the O-H stretching vibrations of the C-OH

groups and water indicaing GO has some water particles entrapped within it. The absorption

bands at 1500 cm^{-1} can be ascribed to benzene rings . The sharp intense peak at 1100 cm-1 can

be attributed to CO carboxylic [41]. At 1720 cm^{-1} (stretching vibrations from C=O), at 1600 cm^{-1}

(skeletal vibrations from unoxidized graphitic domains), at 1220 cm^{-1} (C-OH stretching

vibrations) [40] . Graphene oxide is similar to a graphene sheet with its base having Oxygen-

containing groups. Since these groups have a high affinity to water molecules, it is hydrophilic

and can be easily dissolved in water [41].

NGO –Nitrogen doped graphene (b) in the Fig 4.1 showed all peaks for OH, CH, C=C, C-O and C=O functional groups which have been observed in the GO spectrum. However, there was a peak observed at 1593 cm^{-1} of N-H stretch and it was due to nitrogen which has been introduced into the structure of graphene oxide (GO). Therefore, this confirmed that nitrogen has been successfully doped into the structure of graphene oxide.
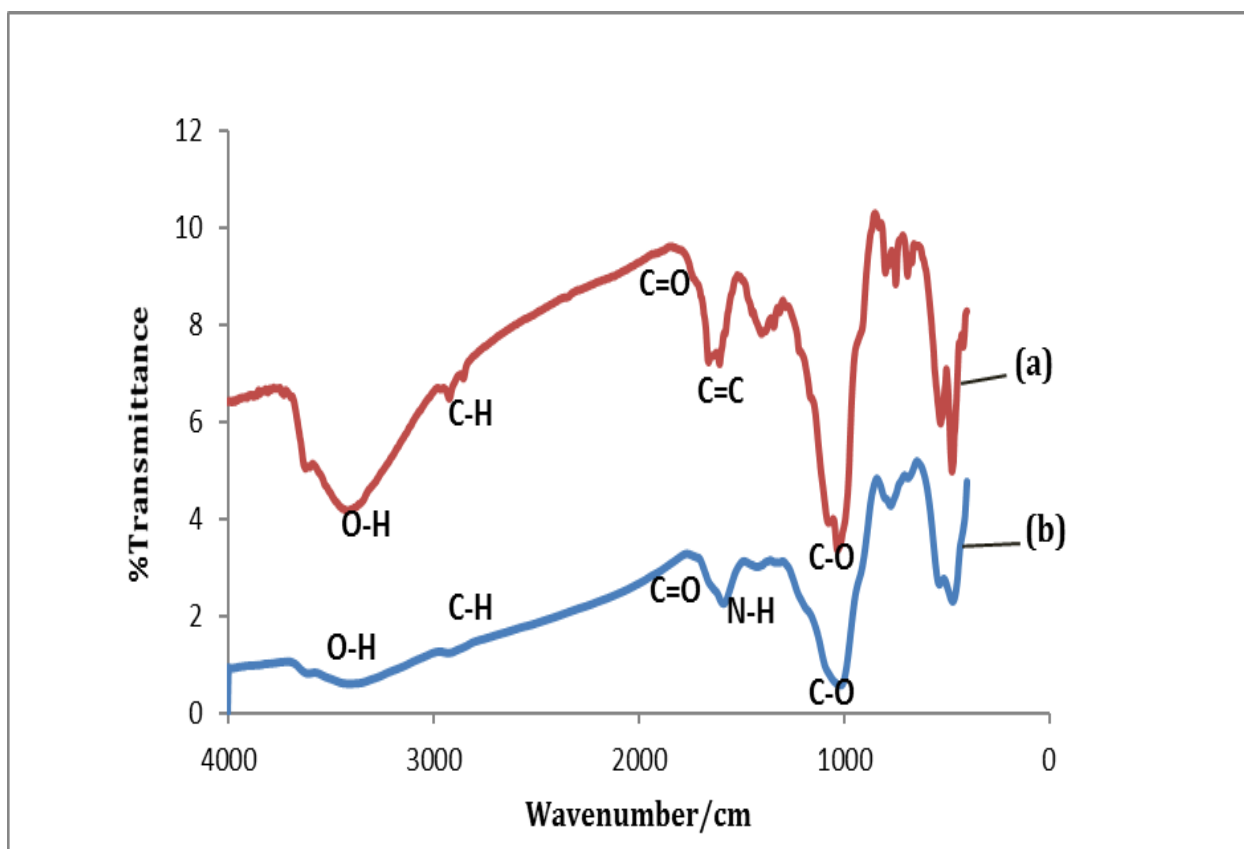
Fig 4.1: Spectrums of graphene oxide (GO) and nitrogen doped graphene oxide (NGO)

4.1.2 FTIR for NITAPC and NITAPC/NDGONS

The FTIR for NITAPC and NITAPC/NGO were obtained in the range of 4000 cm^{-1} to 500 cm^{-1}. Fig 4.2, shows the IR spectra obtained for the NITAPC, which showed peaks at 3443.00 cm^{-1} which is assigned for O-H stretching and peak at 1704.01cm^{-1} is assigned to the C=O. The peaks at 1626 cm^{-1} 1496 cm^{-1} and 1084 cm^{-1}, which coincided with the following bands O – H, C = C, C – C, and C – O respectively. The peak at between 1550 cm^{-1} and 1640 cm^{-1} are assigned for the N-H for the amide group in the metal phthalocyanines.
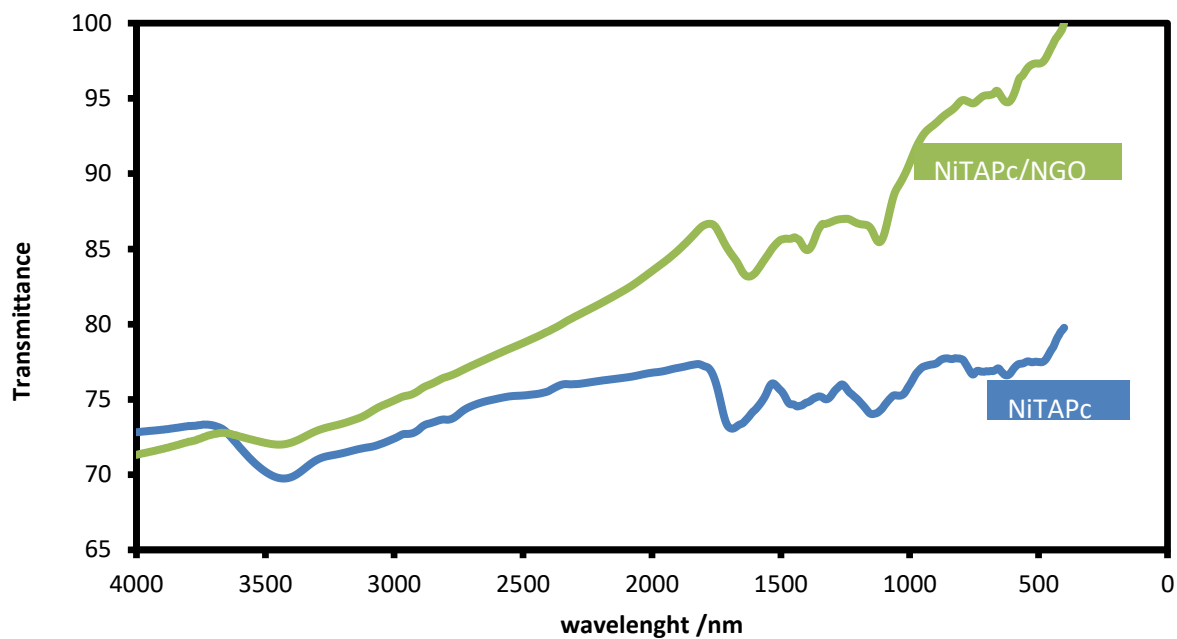
Fig 4.2: FTIR for NITAPC and NITAPC-NDGONS

4.1.3 UV-VIS for NITAPC and NITAPC/NGO

The UV-Vis spectra of NITAPC shows a red shift from 708 nm relative to NITAPC-NGO (mix) whose maxima is 686 nm. Splitting of the Q band which is typical of phthalocyanine is not very clear in the Fig 4.3 ,however there is a broadening which could be either due to low symmetry caused by unresolved splitting or aggregation. The shifting is due to the presence of the pi electron rich carbon which reduce the highest occupied molecular orbital (HOMO) – lowest unoccupied molecular orbital (LUMO) gap of the phthalocyanines[67].
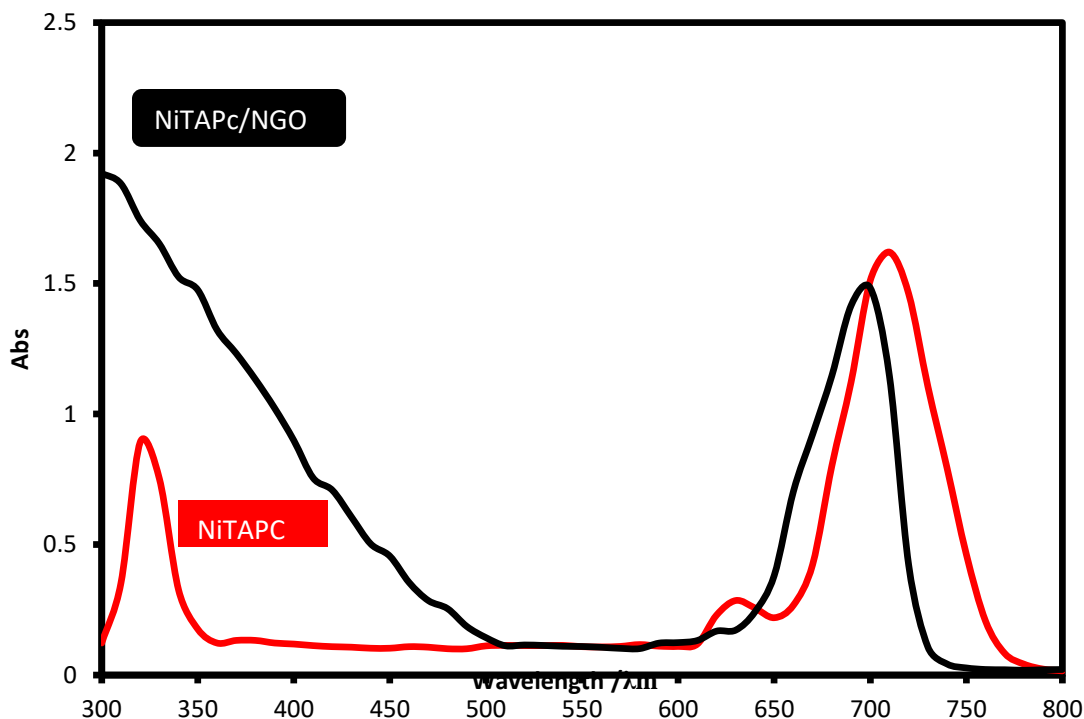
Fig 4.3: UV-VIS for NITAPC and NITAPC-NDGONS

4.2 Cyclic voltammetry

The cathode to anode peak potential separation (ΔEp) for the modifiers used in this study is shown in the Table 4.1. The order in terms of electron transfer efficiency is therefore NDGONS-NiTAPc-GCE (70 mV) > GONS-NiTAPc-GCE (77 mV) > NDGONS-GCE (80 mV) > Bare-GCE (85 mV) > NiTAPc-GCE (117 mV). This confirms the good electron transfer kinetics of NGO-NiTAPc-GCE compared to the rest of the modified electrodes, including the bare GCE. The electron transfer kinetics of the modifiers on the surface of glass carbon were also confirmed by the increase in anodic peak current (Table 4.1), the order of electron transfer is therefore Bare-GCE (I_{Pa}: 25.2 μA) > NiTAPc-GCE (I_{Pa}: 28.2 μA)> NGO-GCE (I_{Pa}: 31.7 μA) > GO-NiTAPc-GCE (I_{Pa}: 34.7 μA) > NGO-NiTAPc-GCE (I_{Pa}: 40.5 μA).

38
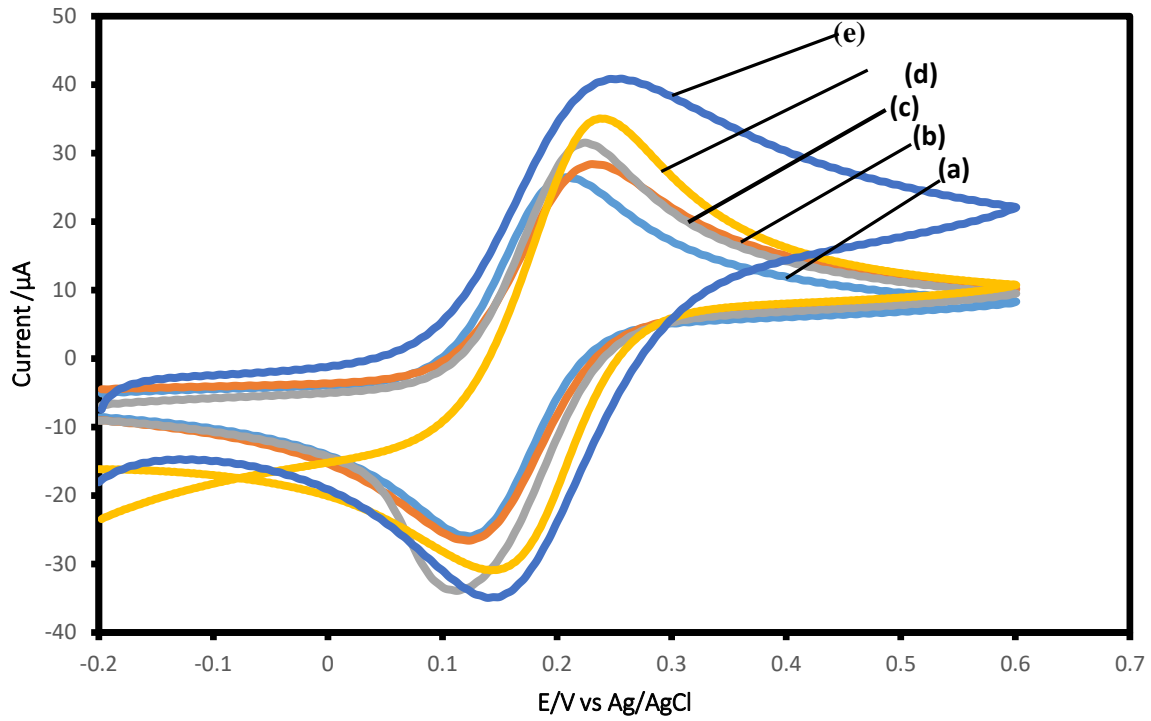
Fig 4.5: Cyclic Voltammograms of bare (a), NiTAPc-GCE (b), NDGONS-GCE (c), GONS-NiTAPc-GCE (d) and NDGONS-NiTAPc-GCE in equimolar solution of ferri/ferro cyanide solution prepared 1 M of KCl.

Table 4.1: Summary parameters obtained from cyclic voltammetry experiments in $[Fe\ (CN)_6]^{3-/4-}$ solution.

Electrodes	Current µA	$\Delta E_{(pa-pc)}(mV)$
Bare -GCE	25.2	85
NiTAPc-GCE	28.2	117
NGO-GCE	31.7	80
GO-NiTAPc-GCE	34.7	77
NGO-NiTAPc-GCE	40.5	70

The lower peak potential separation (77 mV) and high anodic peak current (40.5 µA) for NDGONS-NiTAPc-GCE compared to the rest of the modifiers electrode is possibly due to the linkages between the NiTAPc and NDGONS as well as their good alignment on the electrode surface which makes, electron exchange between the redox probe and electrode modifier much faster confirming its improved electron transfer compared with the rest of the modified electrodes [31].

Also the increase in peak current for NDGONS-NiTAPc–GCE is due to the lone pairs of electron on the nitrogen atom present in the graphene sheets hence resulting in a high increase in delocalized pi electrons within the graphene sheets [32]. The large peak potential separation of 117 mV for NiTAPc-GCE implies that on its own it offers resistance to electron transfer [33], but the high increase in current of NiTAPc as compared to the bare electrode is attributed to the

presence of amine functional groups present on the peripheral groups resulting in the donation of electrons in the phthahlocyanine ring [34]. The electrical properties of NiTAPc is enhanced coupling it with nitrogen doped graphene quantum dots which forms a conjugate through an amide bond facilitating an electron transfer bridge. The enhanced electrical properties of the conjugates was evidenced by increase in current and reduction in potential. The substitution of carbon atoms present in the graphene sheets with atoms such as nitrogen atom results in the enhancement of electrical properties due to the present of lone pairs of electrons on the nitrogen atom [35]. This lone pairs of electrons on the nitrogen atom when delocalized within the pi system of graphene sheets it results in increase in sensitivity and also in the reduction of potential. Substitution of carbon atoms in graphene sheets with foreign atoms results in the change in the configuration of graphene structure hence reducing functional groups such as carboxylic groups making it less soluble in solutions [36]. The carboxyl group on the terminal ends of NGO can interact with amine groups on the NiTAPc hence facilitating the ease of electrons [37].

4.3 Electrochemical Impedance Spectroscopy (EIS)

Electrochemical impedance spectroscopy is a potent tool for the proper determination of both kinetic and mass-transport parameters as well as the charge transfer coefficient [38]. Fig 4.2 shows the EIS response for bare-GCE, NGO-GCE, NiTAPc-GCE, GO-NiTAPc-GCE and NGO-NiTAPc-GCE curves. EIS includes a semi-circular part and a linear part .The semi-circular part at higher frequencies represents the electron-transfer-limited process. The semi-circular diameter is equivalent to the electron transfer resistance which controls the electron transfer kinetics of the redox probe at the electrode interface [39].
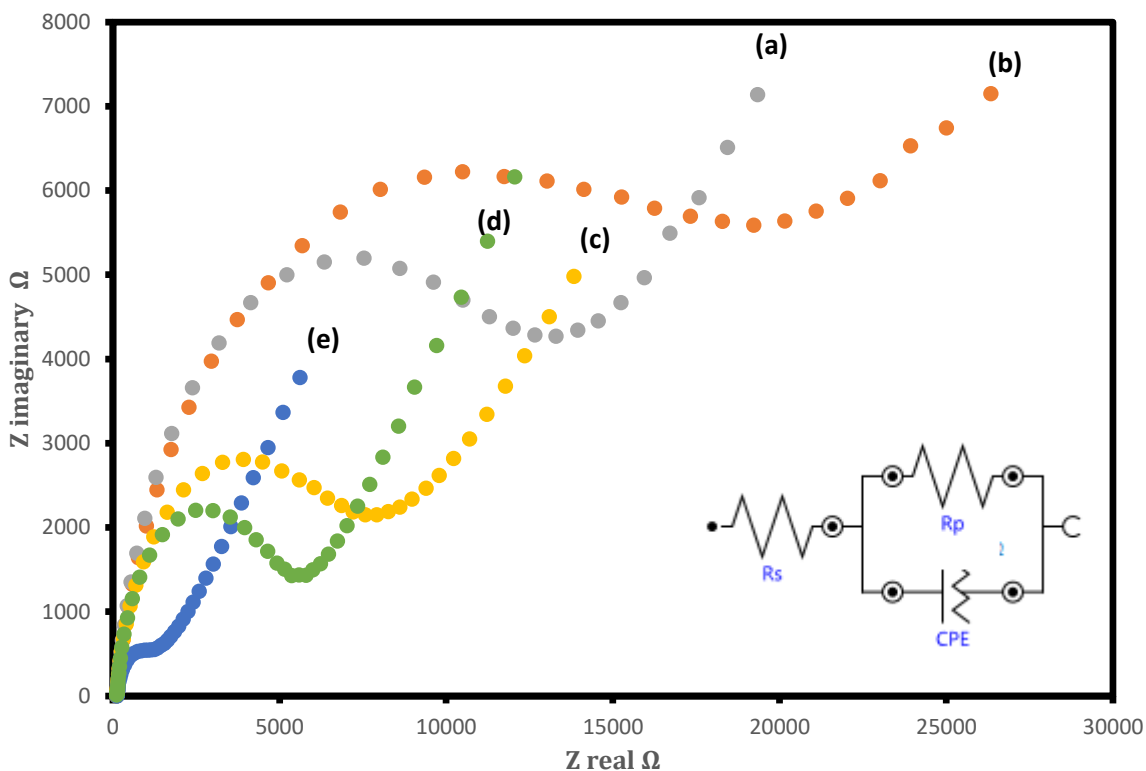
Fig 4.6: Nyquist plots obtained for bare (a), NiTAPc-GCE (b), NDGONS-GCE (c), GO-NiTAPc-GCE (d) and NGO-NiTAPc-GCE in in 1mM [Fe(CN)$_6$]$^{3-/4-}$ solution in 1M of KCl

The properties of surface modified electrodes were revealed by electrochemical impedance spectroscopy. As shown in Fig 4.6 the Rct of NDGONS-NiTAPc-GCE was the smallest during the redox process implying good conductivity. After the less conductive NiTAPc was modified onto the GCE, the RCT increased obviously from 13.29 kΩ (bare) to 19.22 kΩ (NiTAPc) indicating that the electron transfer from the redox probe of [K$_3$Fe(CN)$_6$]to the electrode surface was hindered [52]. When NGO was immobilized on GCE the was a decrease in RCT value from bare (13.29 kΩ) to 7.98 kΩ NGO nanosheets indicating high electron transfer and catalytic properties of the nitrogen doped graphene nanosheets .Moreover the formation of amide linkage between NDGONS and NiTAPc has significantly increased the surface area and enhanced the electrical conductivity of the electrode accounting for the decrease of Rct .The Rct reduced from

19.22 kΩ (NiTAPc) to 1.34 kΩ (NDGONS-NiTAPc-GCE) as nitrogen doped graphene sheets were bonded with the NiTAPc structure suggesting that the impedance of the electrode was decreased . The order of decrease of electron transfer efficiency (in the form of decrease in RCT) is as follows: NDGONS-NiTAPc-GCE > GO-NiTAPc-GCE > NDGONS-GCE>Bare-GCE >NiTAPc. EIS results are in good accordance with CV measurements demonstrating the successful fabrication of the sensor.

The n values where n is an exponent related to depression angle reference are important to mention as they give information about the behaviour of bare and modified electrode surfaces [53]. If the electrode or modified electrode behaves like pure resistor (n=0), Warburg diffusion n=(0.5) and pure capacitor (n=1).The n values ranges from 0.85 to 0.94 and these values are all close to unity (=1) indicating that the electrode behaves like a capacitor .

The RCT can be used to calculate the heterogeneous electron transfer rate constant (kapp) across the electrode interface under study. The RCT is inversely proportional to (kapp) constant, in according to the Equation[54]:

$$kapp = RT/FRCTC \qquad (4.0)$$

Where C is the concentration ($[Fe(CN)_6]^{3-/4-}$1.0 x 10^{-3} mol cm^{-3}), with R and F having their usual meanings the increase in k_{app} value from NDGONS-NiTAPc-GCE (2.05 x 10^{-2} cm s^{-1}) > GO-NiTAPc-GCE (4.332 x 10^{-3} cm s^{-1}) > NDGONS-GCE >(3.23 x 10^{-3} cm s^{-1}) >Bare-GCE (1.92 x 10^{-3} cm s^{-1}) > NiTAPc-GCE (1.27 x 10^{-3} cm s^{-1}),indicating that electron transfer process between the redox and the underlying bare surface are much easier at NDGONS-NiTAPc -GCE compared to other electrodes. The higher k value obtained for the $[Fe(CN)_6]^{3-/4-}$ redox at NGO-NiTAPc-GCE in comparison to other electrode systems indicates that the formation of amide linkage

between NiTAPc and NGO structure facilitates the electron transfer reaction to higher extent as compared to other individual electrodes [55].

4.3 Surface Roughness Factor

The surface roughness factor of the modified electrodes were determined using $[Fe(CN)_6]^{3-/4-}$ redox system and applying the Randles –Sevcik Equation for reversible system [35].

$$I_p= (2.69 \text{ x } 10^5) \text{ } n^{3/2}D^{1/2}CA_{eff}v^{1/2} \hspace{3cm} (4.1)$$

Where Ip the peak current, n is equal to the number of electrons transferred at the surface of the electrode , D is the diffusion coefficient of the analyte in solution 7.6 x 10^{-6} cm^2/s^{-1} and C is the solution concentration in (mol/cm^{-3}),A_{eff} is the effective surface area and v is the scan rate (V/s^{-1}) .The surface roughness factors (ratio of Ipa experimental /Ipa theoretical) were determined for all the probes and the corresponding real electrode areas (roughness factor x theoretical surface area $(=0.072cm^2)$ were determined.

Table 4.2 Electrodes Effective Area

Electrodes	Effective Surface Area/cm^2	Surface roughness factor
Bare -GCE	-	-
NiTAPc-GCE	0.121	1.68
NGO-GCE	0.135	1.88
GO-NiTAPc-GCE	0.148	2.06
NGO-NiTAPc-GCE	0.173	2.41

4.4 Effect of pH

Cyclic voltammetry was used as the electroanalytical tool to observe the current changes as the pH of 0.1 M phosphate buffer solution increased from 3.0 to 8.0, and the test results are illustrated in Fig. 4.3 (A and B). The obtained outcomes indicated that the current values of the anodic peak reached a maximum value at pH 7.0, as shown in Fig. 4.6 (A and B) insets. As a result, 0.1 M phosphate buffer with its pH of 7.0 was assigned as the ideal condition for simultaneous detection of Ascorbic acid and Vanillin. It can be seen in Fig. 4.6 B), the oxidation peak current of ascorbic inreased to maximum values at pH 5 and pH 7, this due to the fact that ascorbic acid has pka values at 4.75 and 6.8 this are due to the deprotonation of H^+ ions of ascorbic into the solution [56]. Hence pH 7 was chosen as an optimum pH in order to detect vanillin and ascorbic acid simultaneously since maximum pH value for vanillin was also pH 7. As can be seen in Fig. 4.6 (C and D), the value of the oxidation peak potential of vanillin and ascorbic acid shifted to more negative potential with the increase in pH from 3 to 8.0, and that it obeys the following equations:

$$E_p \text{ (V)} = -0.0593 \text{ pH} + 0.8827 \text{ (R} = 0.9905) \text{ Vanillin}$$

$$E_p \text{ (V)} = -0.0552 \text{ pH} + 0.5316 \text{ (R} = 0.9965) \text{ Ascorbic acid}$$

A shift of typically 59.3 and 55.2 mV/pH unit is close to the theoretical value of 59 mV/pH unit, indicating that the electron transfer is accompanied by an equal number of protons in electrode reaction [36].
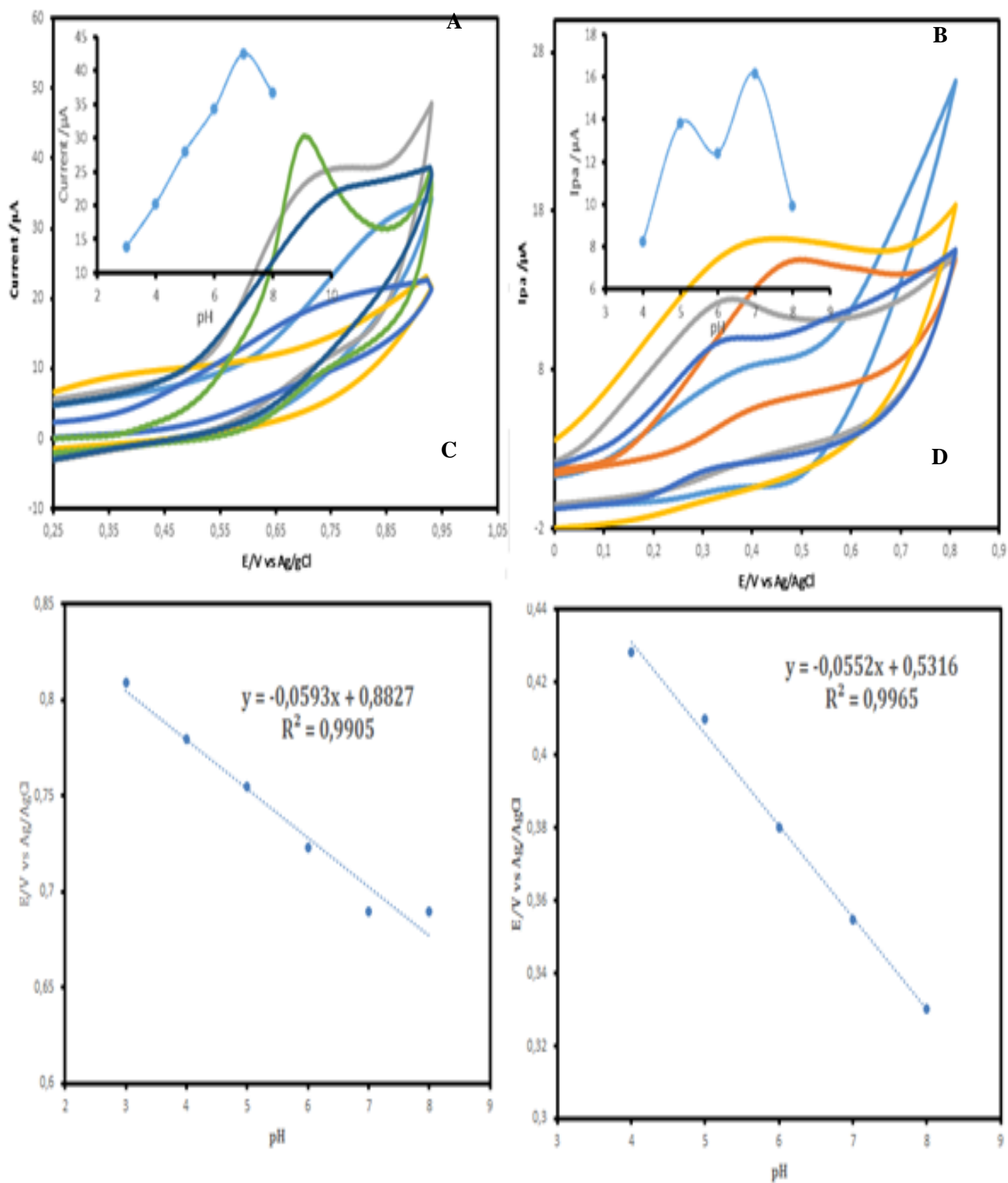
Fig 4.6 (A and B) Cyclic voltammograms of peak currents and peak potentials (A)Vanillin

(B) Ascorbic acid : Fig 4.6 (C and D) plots of potential versus pH values for 1mM Vanillin (C) and

46

1mMAscorbic acid (D), pH 3 to pH 8. Inserts :relationship between the peak currents and pH (Vanillin (A) and Ascorbic Acid (B)

4.5 Electrochemical response of the modified electrodes to vanillin and ascorbic Acid

Comparative studies in 1mM vanillin and Ascorbic acid was carried out for all electrodes bare-GCE, NiTAPc-GCE, NGO-GCE, GO-NiTAPc-GCE and NGO-NiTAPc-GCE in order to observe the reduction in potential and increase in anodic peak current on the electro catalysis of vanillin and ascorbic acid .
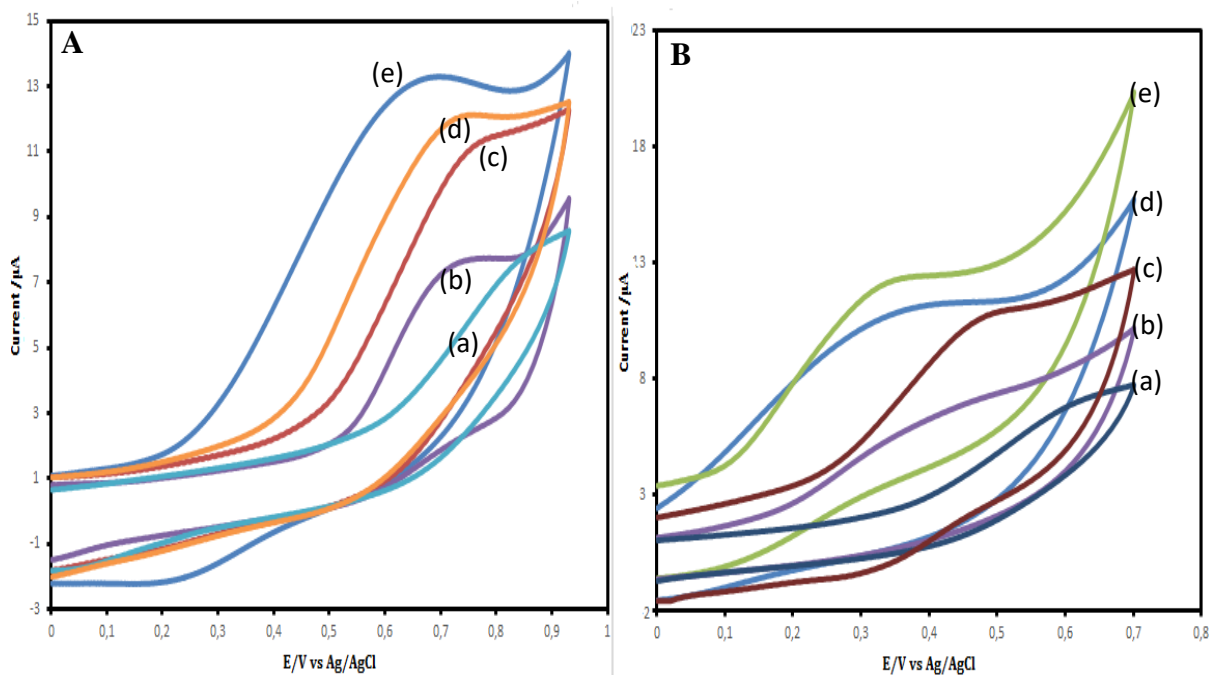
Fig. 4.7 Cyclic voltammograms (A)Vanillin (B)Ascorbic Acid of Bare-GCE (a), NGO-GCE (b), NiTAPc-GCE (c), GO-NiTAPc-GCE (d) and NGO-NiTAPc-GCE (e) in 1mM Vanillin and Ascorbic acid 0.1 M phosphate buffer (pH 7.0).

Fig 4.7 (A and B) indicates peaks of bare GCE are there but not well defined in the potential range with vanillin and ascorbic acid. In the presence of 1 mM Vanillin and ascorbic acid , the NGO-NiTAPc-GCE (e), GO-NiTAPc-GCE (d) , NiTAPc-GCE (c) and NGO-GCE provides a clear oxidation peaks at 0.67 V, 0.70 V, 0.72 and 0.75 V, for vanillin respectively and oxidation peaks for ascorbic acid at 0.30 V ,0.32 V, 0.47 and 0.49V as shown in table 4.4. Furthermore, the oxidation peak currents on NGO-NiTAPc is higher than that of NiTAPc in both analytes, suggesting a stronger electrochemical activity and electron conductivity of NGO-NiTAPc than NiTAPc-GCE[57]. The reasons for the excellent electro-catalytic performance toward Vanillin and Ascorbic acid at NGO-NiTAPc-GCE may be deduced as the following: the numerous catalytic active sites and efficient electrical network for the vanillin and ascorbic acid oxidation are afforded by the chemical link between NGO and NiTAPc forming an amide bond that facilitates electron movement and well-distribution of NGO-NiTAPc arrays on the surface of glass carbon electrode[58]. Also pyridinic N at N-GO can give a pair of electrons for conjugation with the p-conjugated rings, introducing electron donor to NGO and improving the electrochemical behaviors of NGO. Furthermore, the pyrrolic N has higher charge mobility in NGO because of the considerable electron-donor properties and strengthens the carbon catalytic activity in electron transfer reactions[59]. Thus, the electro-catalytic activity of NGO-NiTAPc is trusted to be better than NiTAPc. Without a doubt, the conjugate formed through amide linkage bond of NiTAPc and N-GO makes an excellent electron transfer bridge for the electro-catalytic activity toward the oxidation of vanillin and ascorbic acid.

Table 4.4 Comparative Study of Electrodes in 1 mM Vanillin and Ascorbic acid phosphate buffer solution pH 7.

Electrodes	Currrent µA		Potential V	
	Vanillin	Ascobic acid	Vanillin	Ascorbic acid
Bare-GCE	-	-	6.2	5.2
NGO-GCE	0.75	0.49	7.5	6.9
NiTAPc-GCE	0.72	0.47	11.2	10.6
GO-NiTAPc-GCE	0.70	0.32	11.8	10.9
NGO-NiTAPc-GCE	0.67	0.30	13.2	12.1

4.6 Electrochemical Impedance spectroscopy

Electrochemical impedance spectrum (EIS) is a strong evidence for studying the interface feature of the modified electrodes, which includes a semi-circular portion and a linear portion. The semicircle diameter is corresponding to the electron-transfer resistance (RCT), indicating the electron transfer kinetics of the redox probe [60]. Fig. 4.8 (A and B) displays the impedance spectra of different electrodes in vanillin and ascorbic acid respectively. The bare CPE shows an obvious semicircle (curve c), implying the characteristic of an electron transfer limited process. After modifying the bare electrode with NiTAPc in the electrode, an obvious decrease in semicircle interfacial Ret is obtained (curve d) The RCT of the NGO-NiTAPc-CPE (curve b) is much smaller than those of NGO and NiTAPc/CPE, suggesting that NGO-NiTAPc could serve as a good electron-transfer interface between the electrode and the analytes vanillin and ascorbic acid [61]. Especially, when the NGO-NiTAPc composite was introduced on GCE, we observe that the diameter decreases further (curve a), indicating that the NGO-NiTAPc could more effectively accelerate the electron-transfer, which is ascribed to the synergistic effect of NiTAPc and NGO [39].
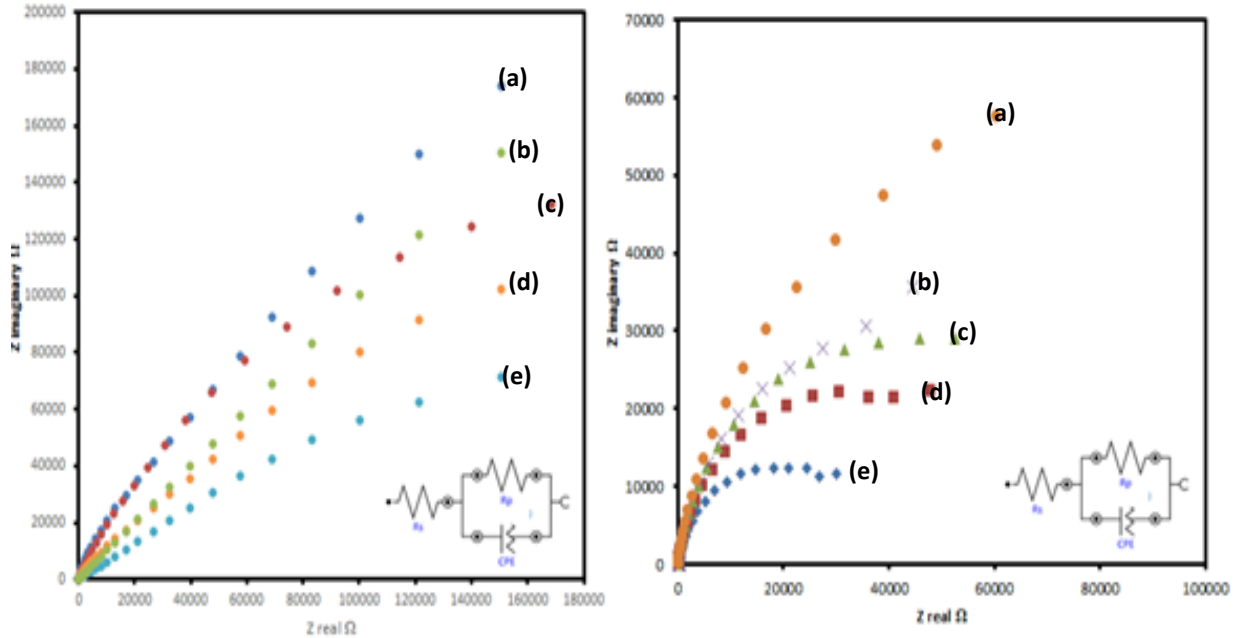
Fig. 4.8 Cyclic voltammograms (A)Vanillin (B)Ascorbic Acid of Bare-GCE (a), NGO-GCE (b), NiTAPc-GCE (c), GO-NiTAPc-GCE (d) and NGO-NiTAPc-GCE (e) in 1mM Vanillin and Ascorbic acid 0.1 M phosphate buffer (pH 7.0).

4.7 Kinetics

The influence of scan rate on the electrochemical response of 1 mM of Ascorbic acid and Vanillin at NGO-NTAPC/GCE was investigated by Cyclic voltammetry in the scan rate range from 50 to 400 mV/s in phosphate buffer solution pH 7 (Fig 4.9 A and B).The results showed that the anodic peak current was increased linearly with the square root rates ($v^{1/2}$), indicating a diffusion controlled electrode process[36]. The linear regression equations of Ascorbic acid and Vanillin (Fig 4.9 A and B insets) are expressed as follows respectively:

$$I_{pa} = 0,6579v^{1/2} + 4,136 \qquad R^2 = 0,9945$$

$$I_{pa} = 10,944v^{1/2} + 8,418 \qquad R^2 = 0,9904$$

Fig 4.9: Effect of scan rate on peak potentials and currents a)50 mV/s, b) 100 mV/s, c) 150 mV/s, d) 200 mV/s, e) 250 mV/s, f) 300 mV/s, g) 350 mV/s and h) 400 mV/s on NGO-NiTAPc for (A) Ascorbic acid (B) Vanillin oxidation. Inset: plot of Current vs √v.
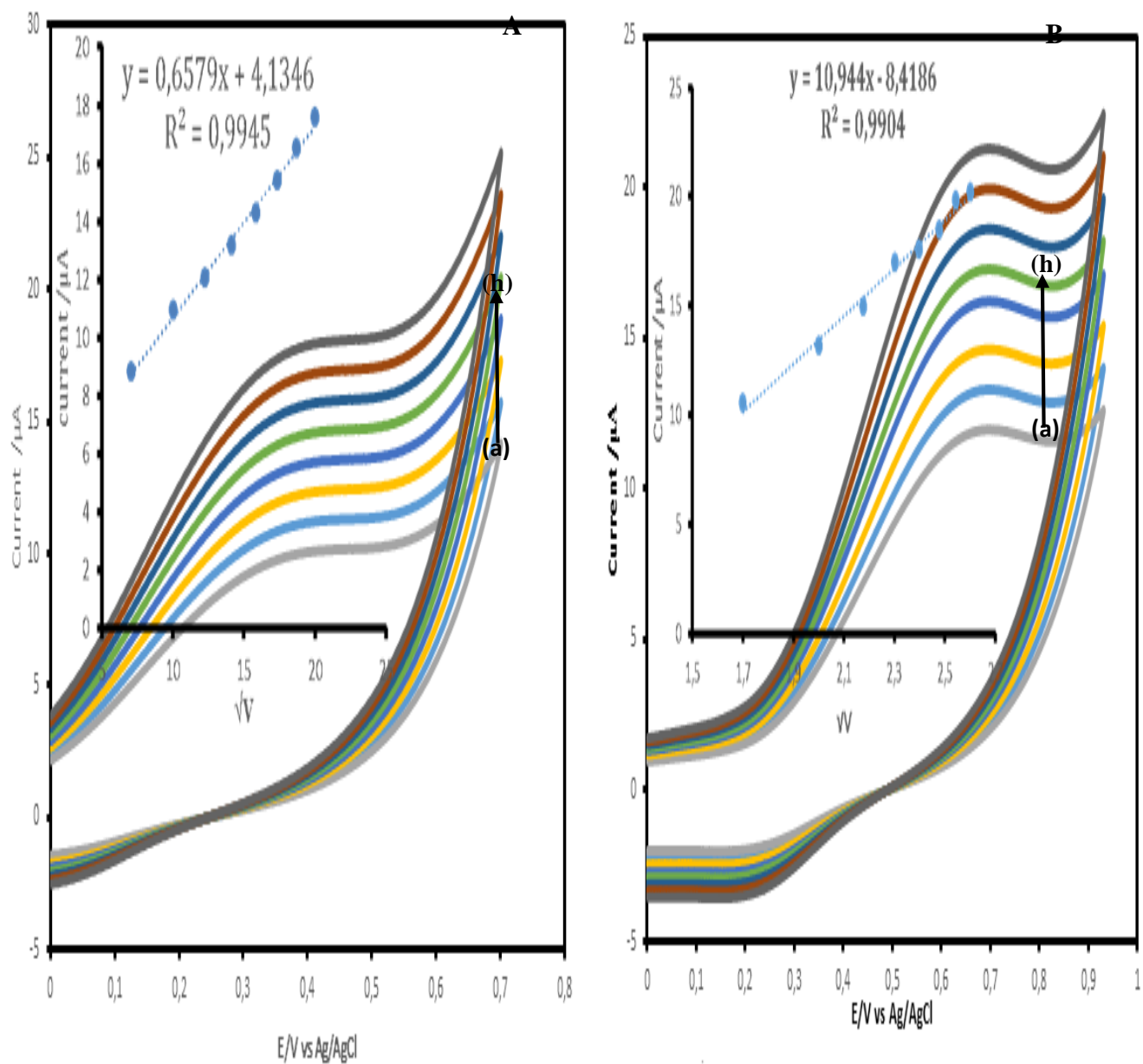
4.8 Tafel Slopes

For an electrochemically irreversible electro-oxidation process the value of Tafel slope (b) can

be obtained from the variation of Epa with v in voltammetric data through equation :

$$E_{pa} = \frac{b(\log v)}{2} + constant \qquad (4.2)$$
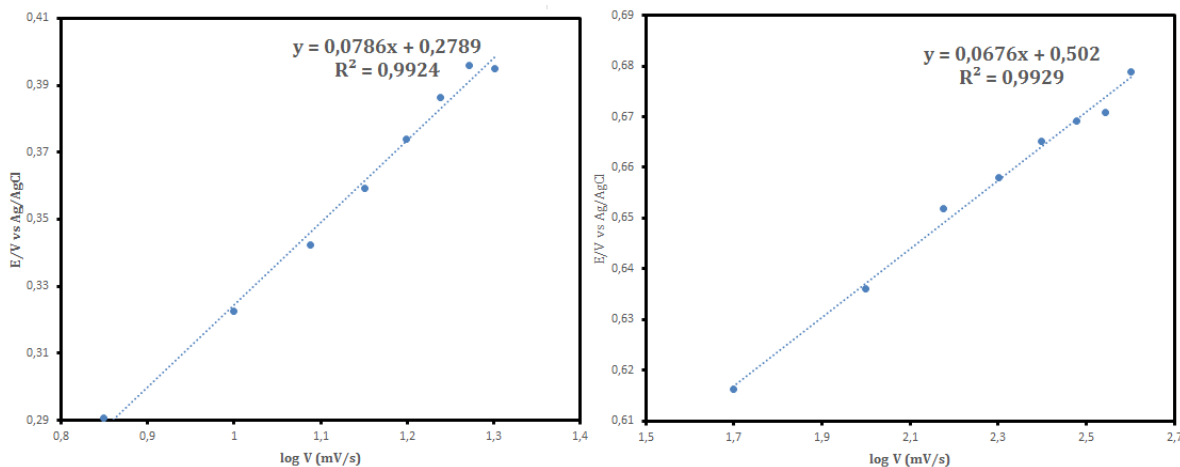
Fig 4.10: Plot of potential versus log scan rate in 1 mM (A) Ascorbic acid and (B) vanillin

The value of b is 2.303RT/(1-α)nₐF and Epa ,α, nₐ and v are the oxidation peak potentials

,electron transfer coefficient ,number of electrons in the rate determining step and scan rate

respectively. The value of Tafel slope gives an idea about the number electrons transferred in the

rate determining step .From the Tafel plot (Fig 4.10) A and B ,value of b for Ascorbic and

Vanillin oxidation were found to be 0.154 and 0.134 respectively at NGO-NiTAPc/GCE. The

value is in close range to the usual range of 0.03-0.120 V

4.9 Order of reaction

The relationship between log Ipa and log concentration was investigated .Linear regression

equations of Ascorbic acid and Vanillin are given below:

$$I_{pa} = 0,5537log\,[Vanillin] + 3,0073 \qquad R^2 = 0,9986$$

$$I_{pa} = 0,569\,log\,[Ascorbic\,Acid] + 2,9689 \qquad R^2 = 0,9979$$

A   B
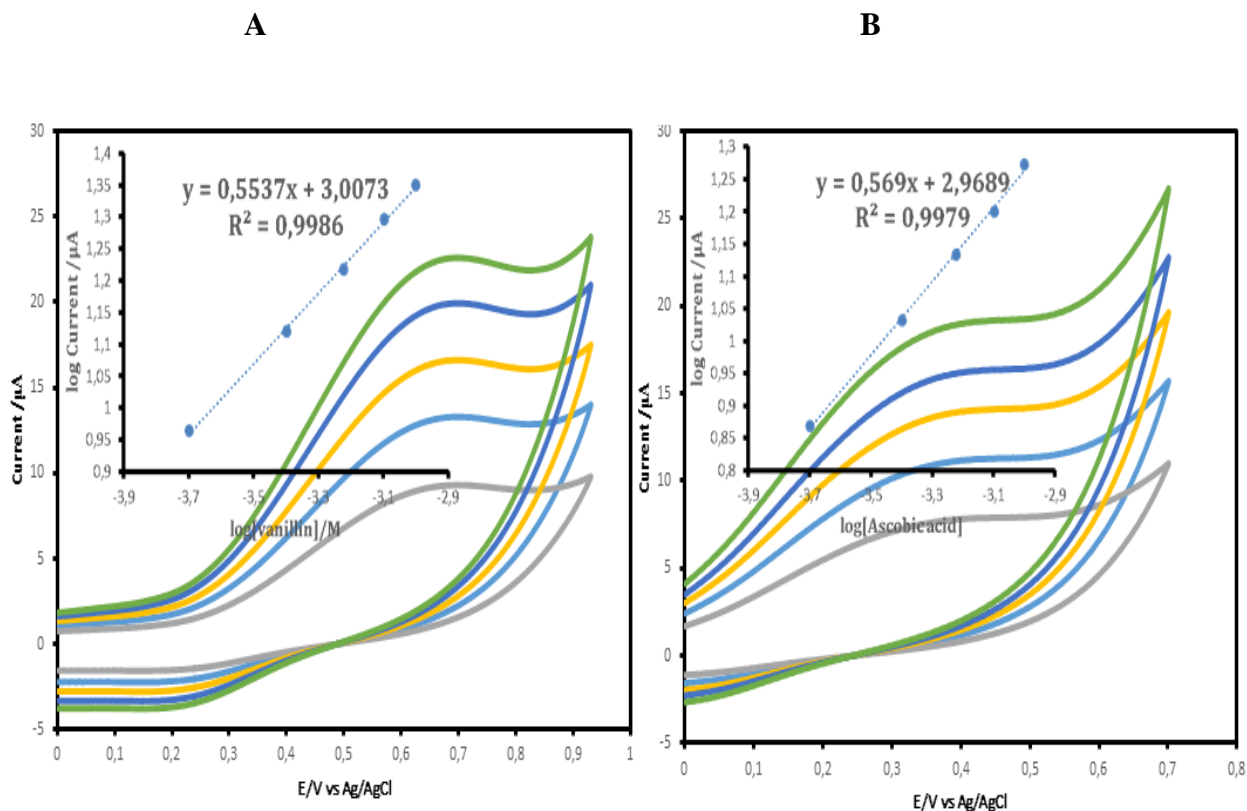
Fig 4.11 Cyclic voltammograms (A) Vanillin and (B) Ascorbic acid for (a) 0.2 mM , (b) 0.4 mM, (c) 0.6 mM (d) 0.8 mM and (e) 1 mM of vanillin and ascorbic acid concentrations in pH 7 PBS. Inset plot of log Ipa vs log [concentration]

According to the slope values, which were equal about 0.5 the electrochemical processes are diffusion controlled [57].The electro catalysis of ascorbic and vanillin was found to be first order from the plot log Current vs log [concentration] (Fig. 4.11 A and B insets), implying that one analyte molecule interacts with one molecule of NDGONS-NiTAPc[62].

4.10 Linear Sweep Studies

Linear sweep voltammetry (LSV) was done to show adsorption behavior of NGO-NiTAPc-GCE.

Fig 4.12 shows LSV plots obtained after keeping the electrode in a stirred solution for 20

minutes to allow for adsorption[35].

$$I_{pa} = 0,5537log \, [Vanillin] + 3,0073 \qquad R^2 = 0,9986$$

$$I_{pa} = 0,569 \, log \, [Ascorbic \, Acid] + 2,9689 \qquad R^2 = 0,9979$$
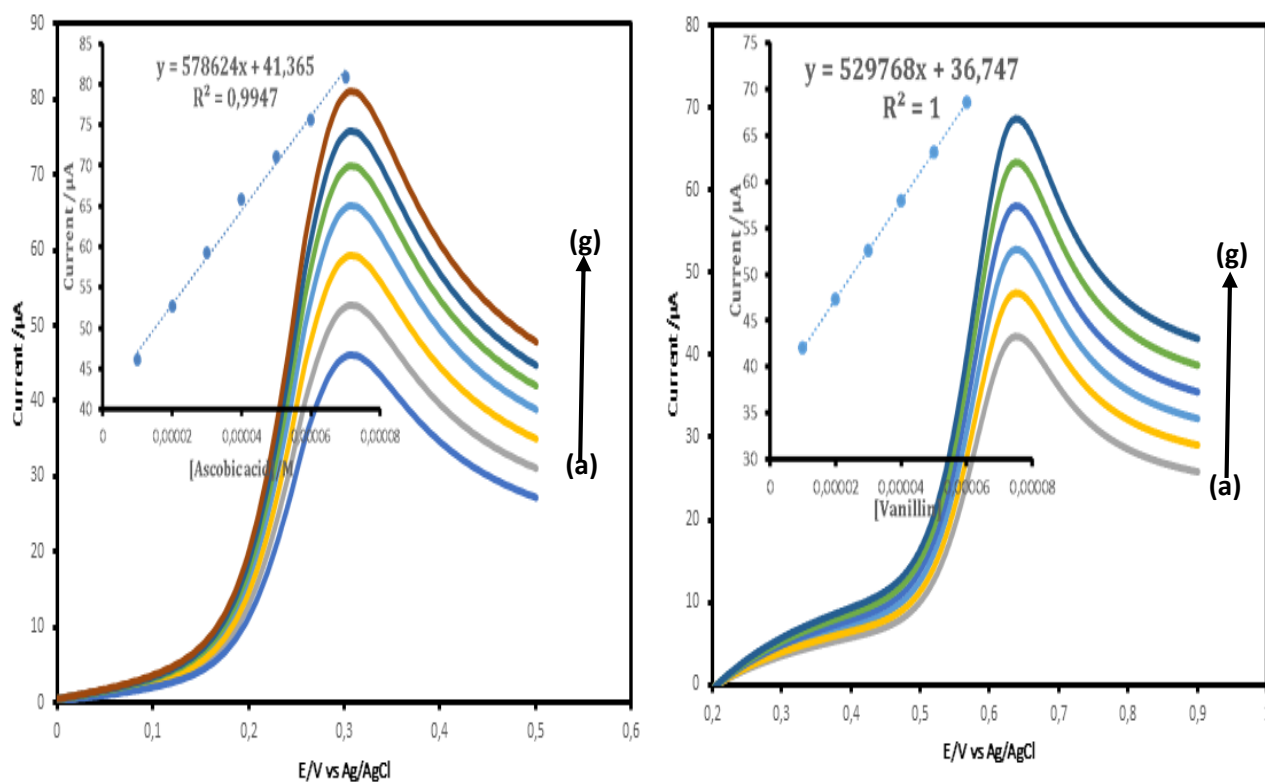
**Fig 4.12 Linear sweep voltammograms (A) Ascorbic acid and (B) Vanillin (a) 10 μM, (b) 20 μM, (c) 30 μM (d) 40 μM, (e) 50 μM, 60 μM and 70 μM of Ascorbic acid and Vanillin concentrations in pH 7 PBS. Inset plot of Current vs. [Concentration].**
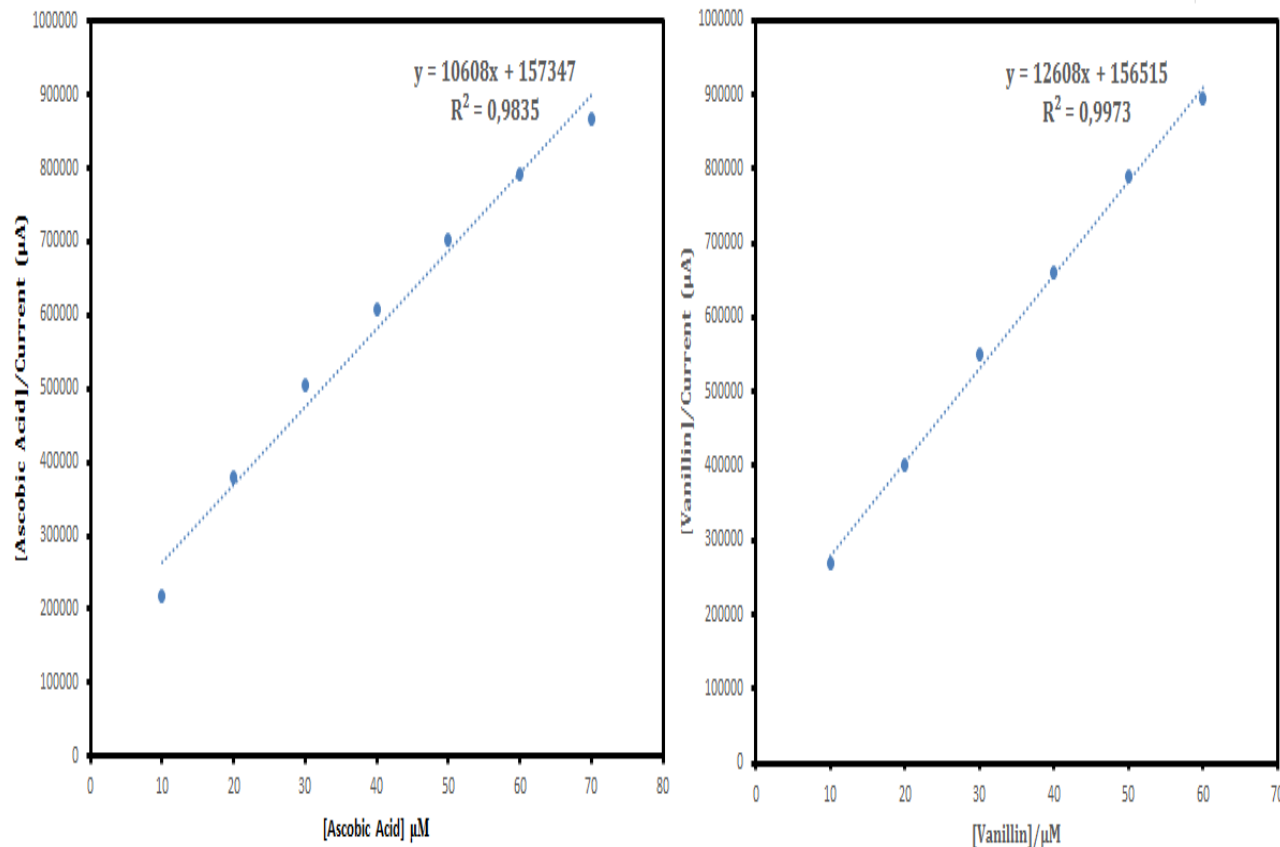
Fig 4.13 Langmuir adsorption isotherm plot for (A) Ascorbic acid and (B) Vanillin on NGO-NiTAPc-GCE in a) 10 μM, (b) 20 μM, (c) 30 μM (d) 40 μM ,(e) 50 μM, 60 μM and 70 μM of ascorbic acid and vanillin concentrations in pH 7 PBS. Oxidation currents employed.

Applying the Langmuir adsorption theory (Eq 4.8) [35], a plot of the ratio of Ascorbic Acid and Vanillin concentration to catalytic current against concentration of Ascorbic acid and Vanillin respectively gave a linear plots which can be interpreted as an adsorption controlled electrochemical process.

$$\frac{[Analyte]}{I_{cat}} = \frac{1}{\beta I_{max}} + \frac{[Analyte]}{I\,max} \tag{4.3}$$

Where [analyte] is the concentration of either vanillin or ascorbic acid

56

where ß is the adsorption equilibrium constant, I_{max} is the maximum current and I_{cat} is the catalytic current. From the slope and the intercept of Fig 4.13 the adsorption equilibrium constant ß for Ascorbic Acid and Vanillin was established to be 6.4 x 10^2 M^{-1} and 8.05 x 10^2 M^{-1} respectively. Using equation 4.9 which relates Gibbs free energy change due to adsorption (ΔG°) the adsorption equilibrium constant ß, (ΔG°) for Ascorbic acid and Vanillin was found to be -16.01 kJ and -16.57 kJ respectively. This value is in comparable to those reported elsewhere for high Tafel slopes [35].

$$\Delta G^{\circ} = -RT \ln \text{ß} \qquad (4.4)$$

Where R is the molar gas constant and T is room temperature

4.11 Chronoamperometry Studies

Chronoamperometry data was used to determine catalytic rate constant for the oxidation of Ascorbic Acid and Vanillin (Fig 4.14 A and B). Catalytic rate constants are a measure of how fast redox processes takes place at the electrode /analyte interface[54].
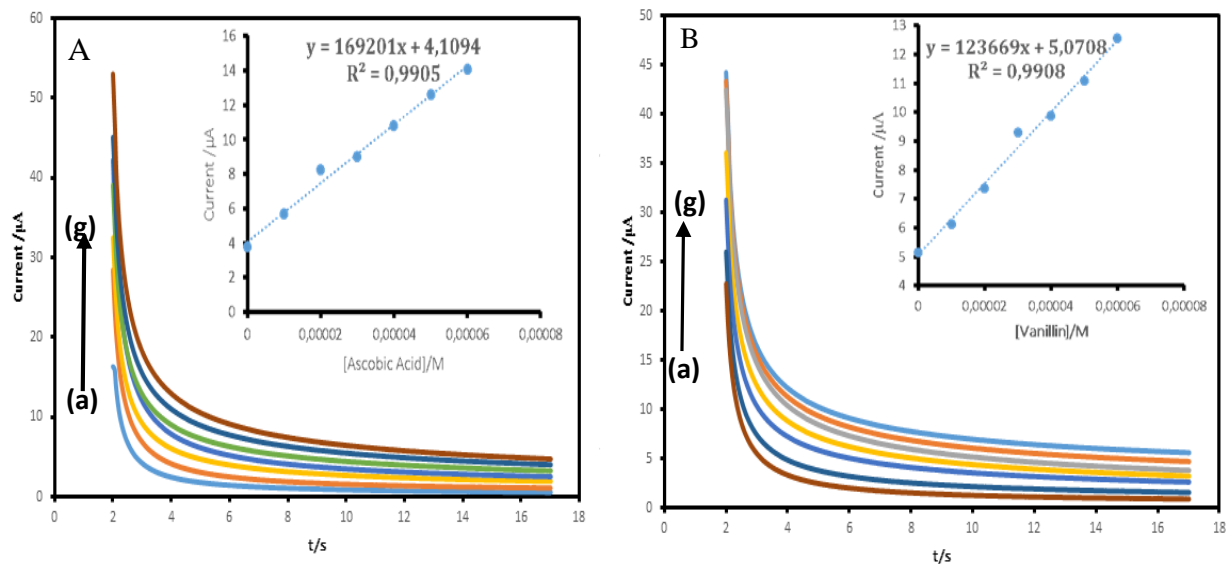
Fig 4.14: Chronoamperograms for different (A) Ascorbic acid and (B) Vanillin concentrations. In PBS pH 7 a), 10 µM b) , 20 µM c) , 30 µM d) , 40 µM e) , 50 µM f) and 60 µM g). *Inset* **Current vs [Ascorbic acid] (A) and [Vanillin] (B)**
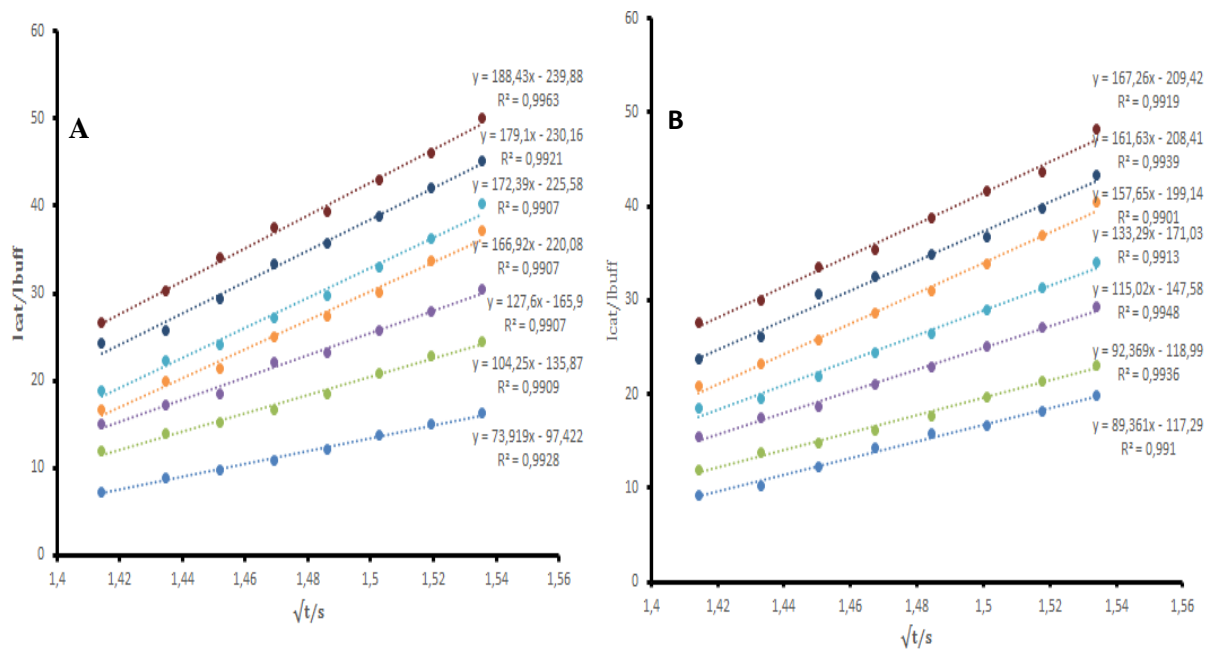
Fig 4.15 Plots of I$_{cat}$/I$_{buf}$ vs time (s) (A) Ascorbic Acid and (B) Vanillin
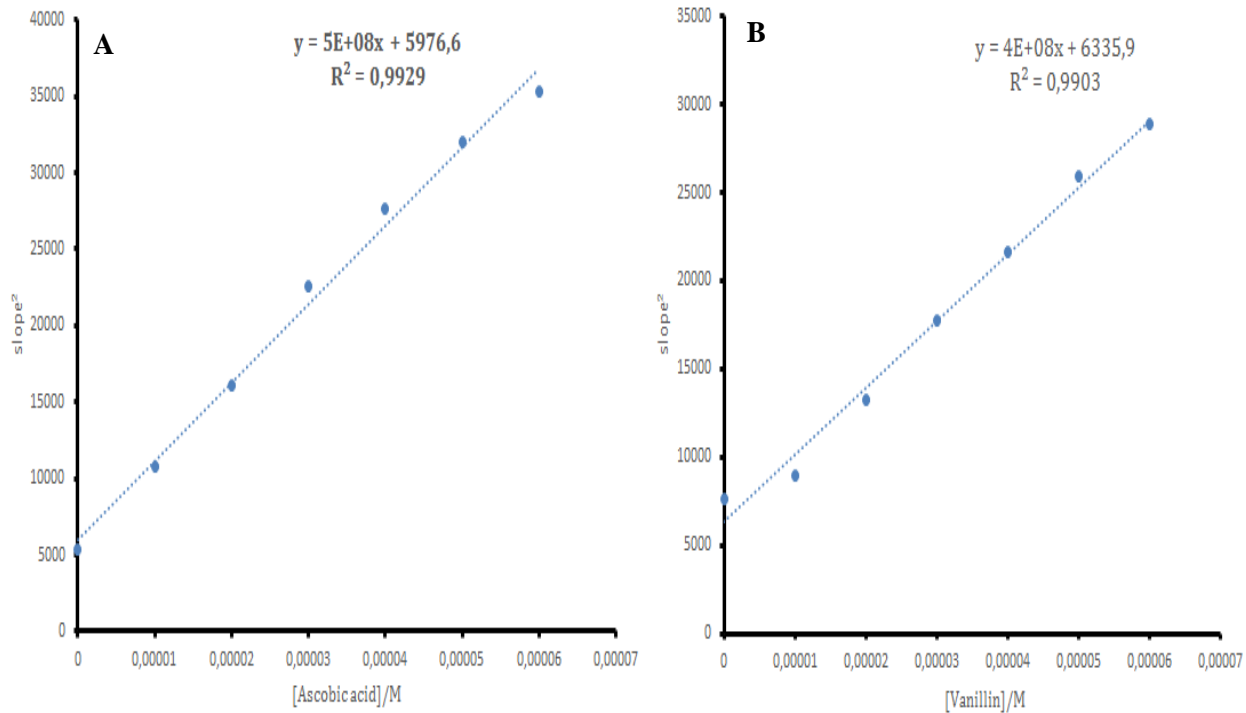
Fig 4.16 Plot of slopes^2 vs. [Ascorbic Acid] (A) and (B) [Vanillin]

The rate constant for the detection of Ascorbic Acid and Vanillin was calculated using the equation:

$$\frac{I_{cat}}{I_{buf}} = \pi^{\frac{1}{2}}(kC_0t)^{1/2} \qquad\qquad (4.5)$$

Where I_{cat} and I_{buf} are currents in the presence and in the absence of Ascorbic Acid and Vanillin, k is the catalytic constant ($M^{-1}s^{-1}$) for the Ascorbic acid and Vanillin oxidation and t is the time in seconds. Figure 4.15 (A and B). Shows the linear relationship for the I_{cat} and I_{buf} vs $t^{1/2}$ plots for different concentrations obtained from the chronoamperograms. Fig 4.16 (A and B) showed the linear relationship for the slope^2 vs. [Ascorbic Acid]/ [Vanillin]. The slopes of Figure 4.16 A and B are equal to πk and this gives k values of 1.59 x 10^8 $M^{-1}s^{-1}$ for Ascorbic acid and Vanillin 1.28 x 10^8 $M^{-1}s^{-1}$.

Figure 4.14 (A) insets shows the oxidation peak current was proportional to ascorbic acid concentration in the range of between 10 to 70 μM with $r^2 = 0.9905$. The limit of detection is equivalent to $3\sigma/s$ where σ is the standard deviation of the intercept and s is the slope of the calibration curve. LoD for ascorbic acid was found to be 7.09 x 10^{-6} M. The LOQ ($10\sigma/s$) was found to be 2.15 x 10^{-5} M. The inset in Fig. 4.14 (B) illustrates that the peak current increases linearly with vanillin concentration between 10 to 70 μM with $r^2 = 0.9908$. The low detection limit is 7.64 x 10^{-6} M for vanillin (S/N = 3) and limit of quantification was 2.32 x 10^{-5} M (S/N = 10).

4.12 Impedimetric sensor for Vanillin determination

In order to develop an impedimetric sensor, EIS measurements were performed at the NDGONS-NiTAPc film in the presence of various vanillin concentrations.
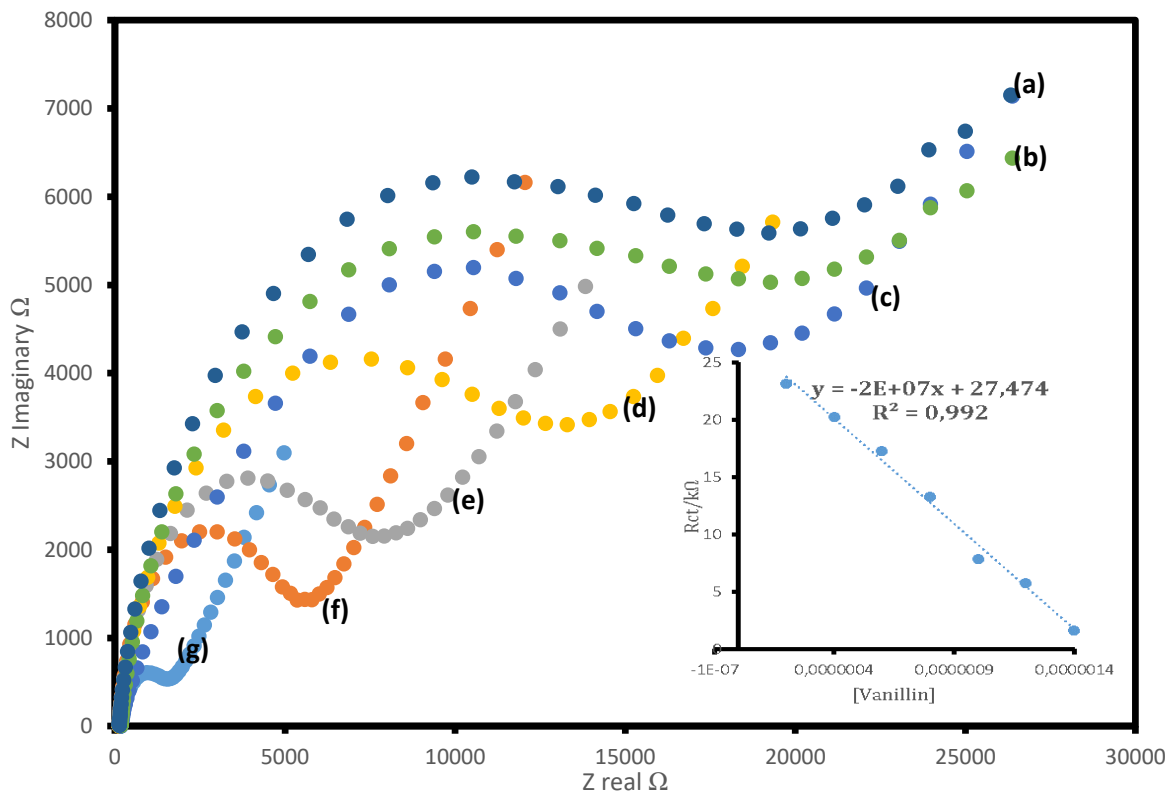
Fig 4.17: Impedimetric response obtained at NDGONS-NiTAPc-GCE in presence of various vanillin concentrations from 0.2 mM (a) - 1.4 mM (g) in 0.1MPBS pH 7.0.

The obtained Nyquist plots are shown in Fig.4.17. In the Nyquist plots, the semicircles from inner to outer are the impedimetric responses obtained at NGO-NiTAPc-GCE for 0.2 Mm – 1.4 mM vanillin (a-g) concentration additions. It is clear that the semicircle diameter increased with increase in vanillin concentration additions. Figure 4.17 (A) insets shows the RCT was proportional to vanillin concentration in the range of between 10 to 70 μM with r^2 = 0.9992. The limit of detection is equivalent to $3\sigma/s$ where σ is the standard deviation of the intercept and s is the slope of the calibration curve. LoD for vanillin was found to be 1.45 x 10^{-7} M. The LOQ $(10\sigma/s)$ was found to be 4.42 x 10^{-7} M.

4.13 Differential Pulse Voltammetry

Under the optimal conditions, differential pulse voltammetry (DPV) was used to determine vanillin and ascorbic acid due to its higher sensitivity than cyclic voltammetry[63]. Fig. 4.18 (A and B) shows the differential pulse voltammograms of different concentrations of vanillin and ascorbic acid in pH 7.
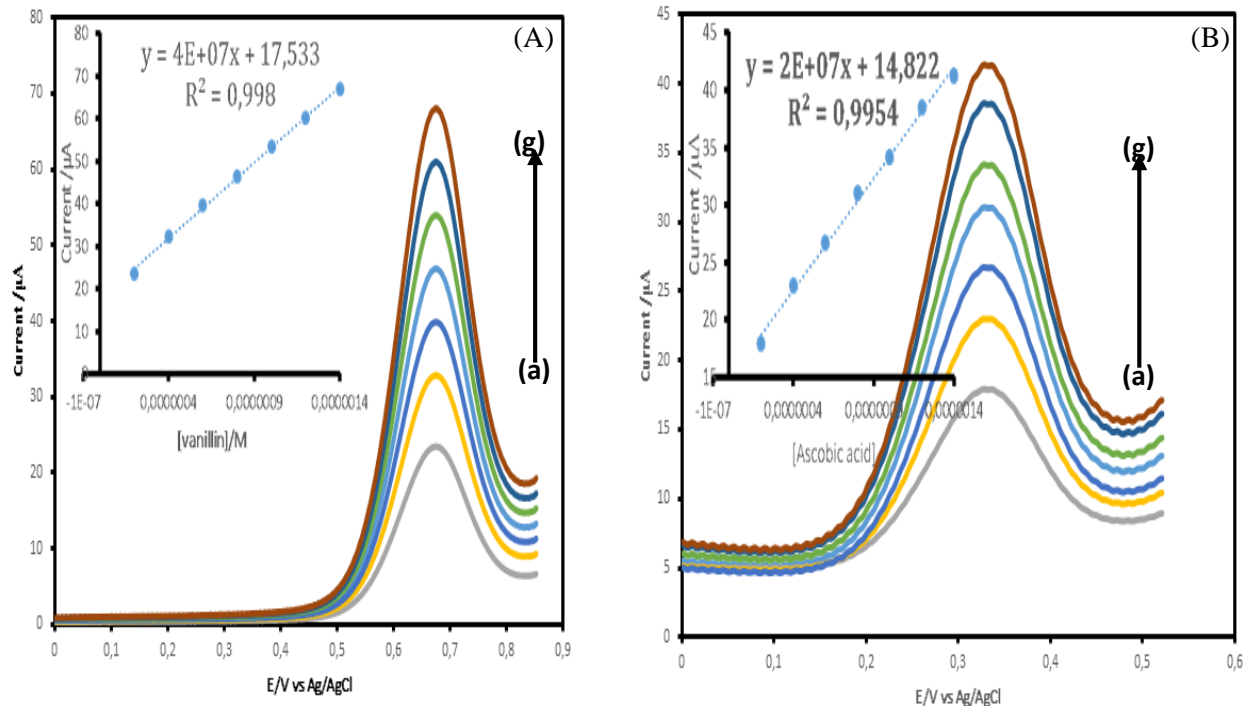
Figure 4.18 (A and B) DPV for NGO-NiTAPc-GCE in: a) 0.2 µM, b) 0.4 µM, c) 0.6 µM, d) 0.8 µM, e) 1 µM, f) 1.2 µM, g) 1.4 µM, h) . *Inset***: Plot of Current vs [ascorbic acid]/[vanillin]**

As can be seen in the inset of Fig. 4.18 (A) , the oxidation peak current was proportional to vanillin concentration in the range of between 0.2 and 1.4 µM with r^2 = 0.998. The limit of detection is equivalent to $3\sigma/s$ where σ is the standard deviation of the intercept and s is the slope of the calibration curve. LoD for vanillin was found to be 2.58 x 10^{-8} M. The LOQ ($10\sigma/s$) was found to be 6.8 x 10^{-8} M. Fig 4.15 (B) The inset shows that the peak current varies linearly with ascorbic acid concentration between 0.2 and 1.4 mM with r^2 = 0.9954. The limit of detection is equivalent to $3\sigma/s$ where σ is the standard deviation of the intercept and s is the slope of the calibration curve. LOD for ascorbic acid was found to be 8.6 x 10^{-8} M. The LOQ ($10\sigma/s$) was found to be 2.6 x 10^{-7} M.

4.14 Simultaneous detection

Fig 4.19 shows the simultaneous cyclic voltammograms obtained on NGO-NiTAPc/GCE composite film modified GCE in equimolar solution of ascorbic acid and vanillin at different scan rates. Fig 4.19 insets shows variation of peak intensities as a function of $v^{1/2}$ the equations fit well to a straight line Fig 4.19 for oxidation process and is indicative of mass transfer controlled oxidative electron transfer[64]. The equations are given below:

$$I_{pa} = 0,893\,v^{1/2} + 8,4964 \qquad R^2 = 0,9986 \quad \text{Vanillin}$$

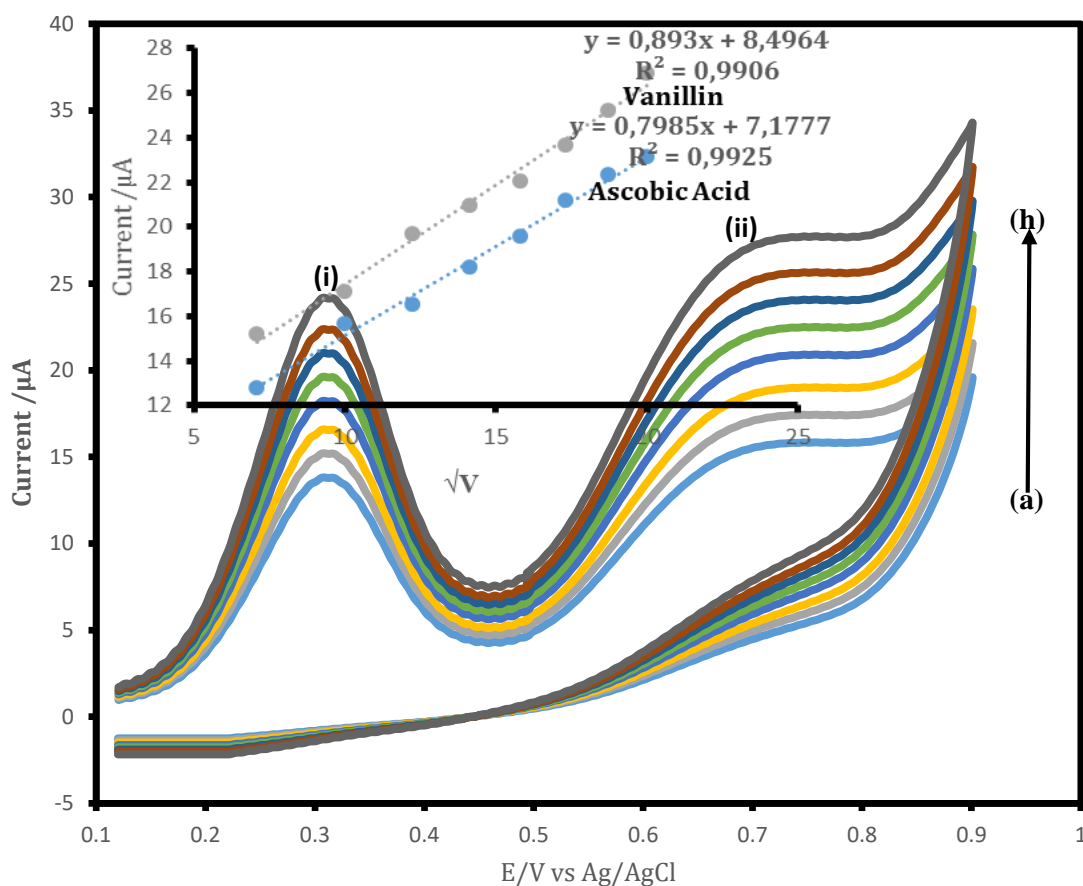$$I_{pa} = 0,7985\,v^{1/2} + 7,1773 \qquad R^2 = 0,9986 \quad \text{Ascorbic Acid}$$

Fig 4.19: Simultaneous Cyclic voltammograms for the detection of equimolar solution of (i) Ascorbic acid and (ii) Vanillin at different scan rates(a) 50 mV/s, (b) 100 mV/s, (c) 150 mV/s, (d) 200 mV/s, (e) 250 mV/s, (f) 300 mV/s and (g) 350 mV/s and (h) 400 mV/s on NGO-NiTAPc/GCE. Insets show plot of Current vs.$v^{1/2}$ (scan rate).

On increasing the scan rates, the peak currents and peak separation increased linearly. Meanwhile, the cathodic peak potentials showed a small shift and the peak-to-peak separation also increased. The anodic peak currents increased linearly with scan rates from 50 to 400 mV/s. A linear plot of current versus root of scan rate confirmed that the irreversible catalytic oxidation of Vanillin and Ascorbic acid is diffusion controlled.

4.15 Simultaneous Detection of Ascorbic Acid and Vanillin

DPV was used to determine the linear ranges and the detection limit of Vanillin and Ascorbic acid at NGO-NiTAPc/GCE .The use of DPV was based on the fact that it has a much higher current sensitivity than cyclic voltammetry. For simultaneous and quantitative determination of ascorbic acid and vanillin, DPV curves at different concentrations of ascorbic acid were recorded in Fig. 4.20 A, where ascorbic acid concentration was kept at 0.2 μM The inset shows that the peak current varies linearly with vanillin concentration between 0.2 and 1.4 μM with r^2 = 0.995. Importantly, the anodic peak current of ascorbic acid is almost uninfluenced by the increase of vanillin concentration, suggesting that oxidations of ascorbic acid and vanillin at the NGO-NiTAPc-GCE are independent of each other. With the DPV technique the detection limit of vanillin is 1.582 x 10^{-8} M in the presence of 0.2 μM ascorbic acid interference (S/N = 3) and limit of quantification was calculated to be 4.55 x 10^{-8} M (S/N = 10) . Fig. 4.20 B presents DPV responses at different concentrations of ascorbic acid while vanillin is kept constant at 0.2 μM. Similar to the scenario in Fig.4.20 A, the anodic peak current of vanillin stays almost constant as

ascorbic acid concentration is increased gradually, further confirming that this modified electrode can be employed for simultaneous determination of ascorbic acid and vanillin. The inset in Fig. 4.20 illustrates that the peak current increases linearly with ascorbic acid concentration between 0.2 and 1.4 µM with r^2 = 0.995. In the presence of ascorbic acid, the low limit is 1.162×10^{-7} M for ascorbic acid (S/N = 3) and limit of quantification was 3.52×10^{-7} M (S/N = 10).
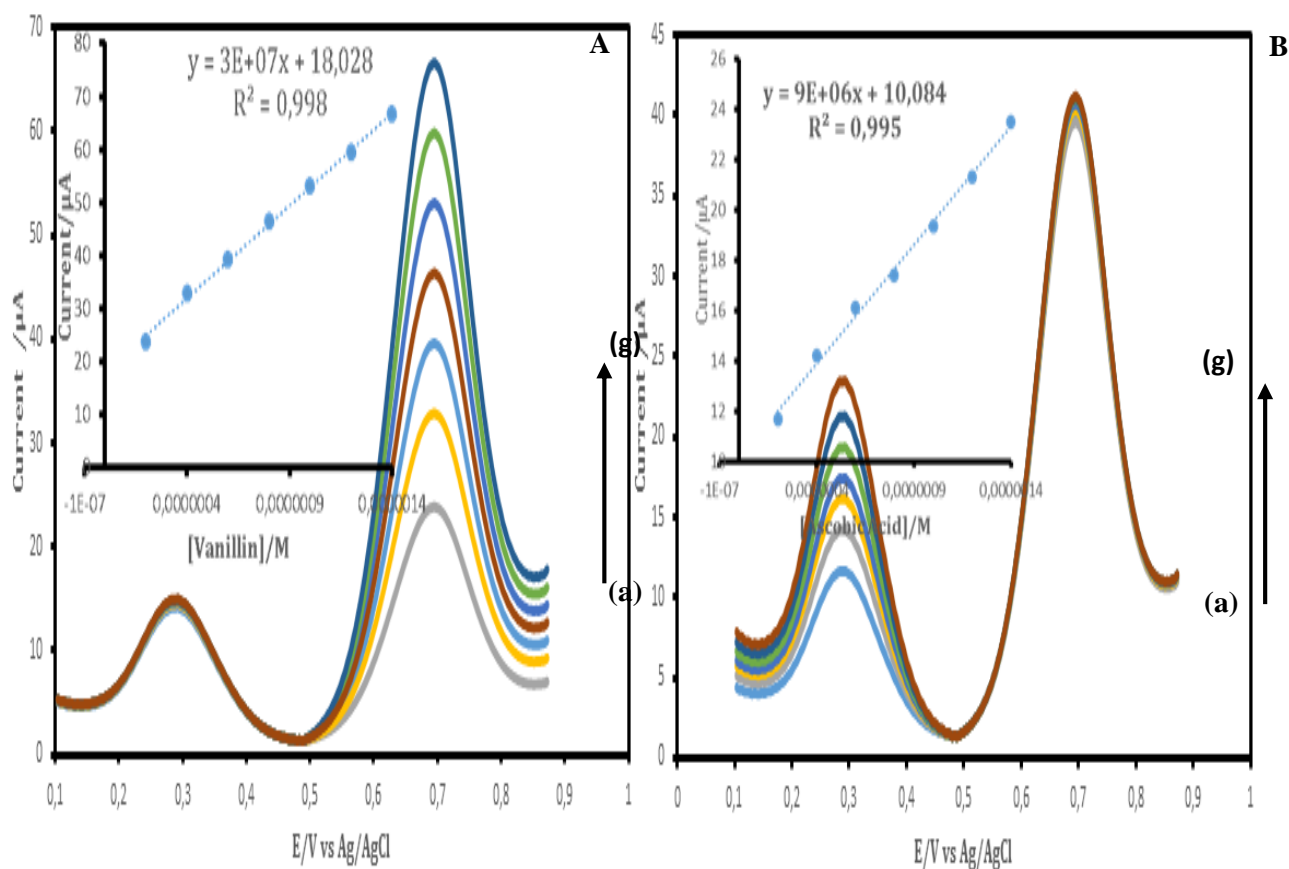
Figure 4.20 Simultaneous DPV for (A) Vanillin and (B) Ascorbic Acid at NGQD-NiTAPc-GCE in: a) 0.2 µM, b) 0.4 µM, c) 0.6 µM, d) 0.8 µM, e) 1 µM, f) 1.2 µM, g) 1.4 µM. *Inset*: Plot of Ipa vs [Vanillin]/ [Ascorbic acid].

4.16 Effect of increasing concentration towards simultaneous detection of vanillin and ascorbic acid
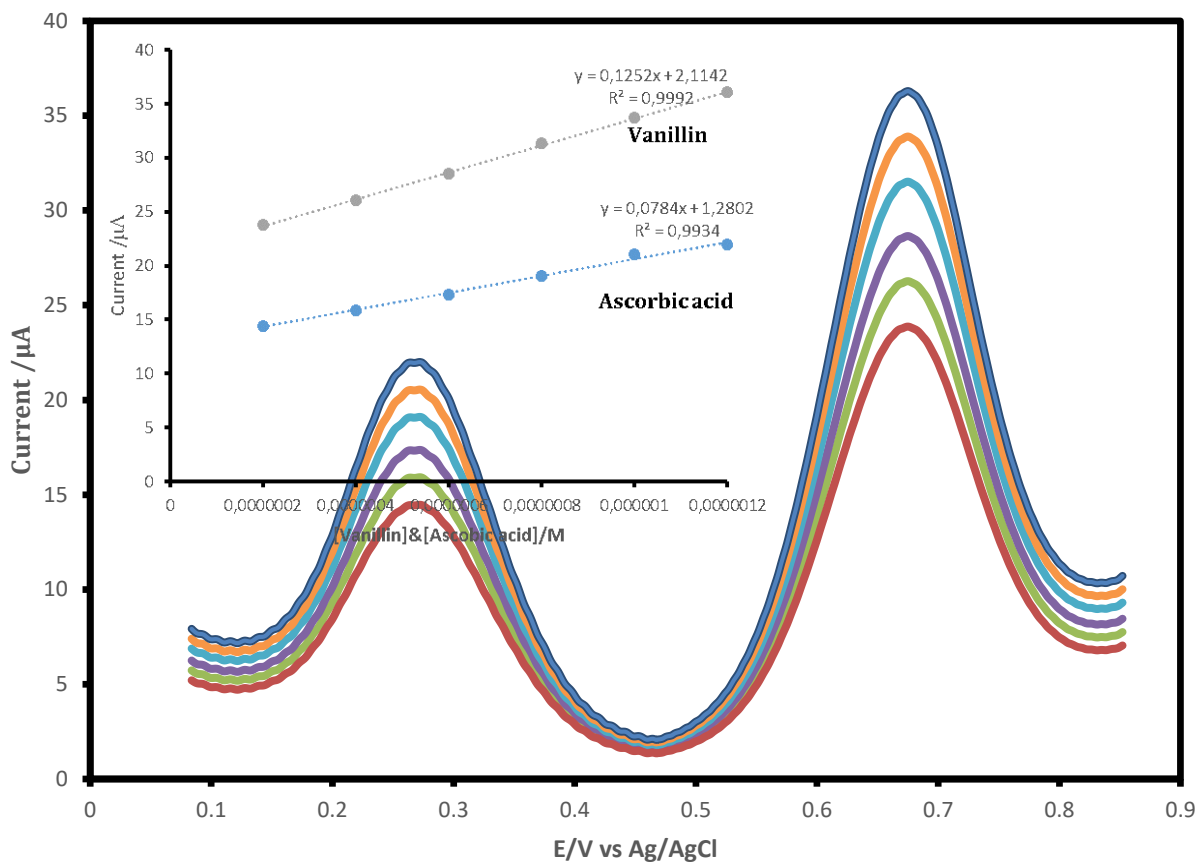
Fig 4.21 Simultaneous DPV for Vanillin and   Ascorbic Acid at NGQD-NiTAPc-GCE in: a) 0.2 µM, b) 0.4 µM, c) 0.6 µM, d) 0.8 µM, e) 1 µM, f) 1.2 µM, g) 1.4 µM. *Inset*: Plot of Ipa vs [Vanillin]/ [Ascorbic acid].

The effect of increasing concentration was investigated on NDGONS-NiTAPc-GCE for the simultaneous determination of ascorbic acid and vanillin. As shown in Figure 4.21 two well distinguished oxidation peaks are observed , indicating that the catalytic reactions of Vanillin and Ascorbic acid at NDGONS-NiTAPc-GCE occur independently ,The oxidation peak currents of

Ascorbic acid and Vanillin increase linearly with their concentration in the range from 0.2 – 1.4 µM .The regression equations are given below :

$$\frac{I_{pa}}{\mu A} = 0,893\ C\ + 8,4964\ R^2 \qquad\qquad = 0,9986\ \text{Ascorbic acid}$$

$$\frac{I_{pa}}{\mu A} = 0,893\ C\ + 8,4964\ R^2 \qquad\qquad = 0,9986\ \text{Vanillin}$$

Thus the results demonstrate that Ascorbic acid and Vanillin can be selectively determined by NDGONS-NiTAPc-GCE without interference from each other.

4.17 Stability studies for ascorbic and vanillin

Figure 4.22 A and B shows a 20 cycle continuous scan voltammograms for NGO-NiTAPc-GCE in 1mM Ascorbic acid and Vanillin respectively. The stability of the modified electrode towards the detection of ascorbic acid indicated that the electrode remained almost constant during the experiment indicating that there was no signal loss for the sensor towards the detection of Ascorbic acid. The electrode stability for the detection of vanillin was confirmed by noting the drop in current from scan 1 to scan 2. A percentage decrease of 1.95 % was observed from the first scan to the second scan. Drop in current is a passivation phenomenon and the rate at which the current drops is a measure of resistance to passivation of the electrode towards that analyte [64]. The percentage decrease of 1.95 % from the first scan to the second scan shows that the NGO-NiTAPc was not very stable. Passivation was attributed to vanillin and its interaction with the electrode.
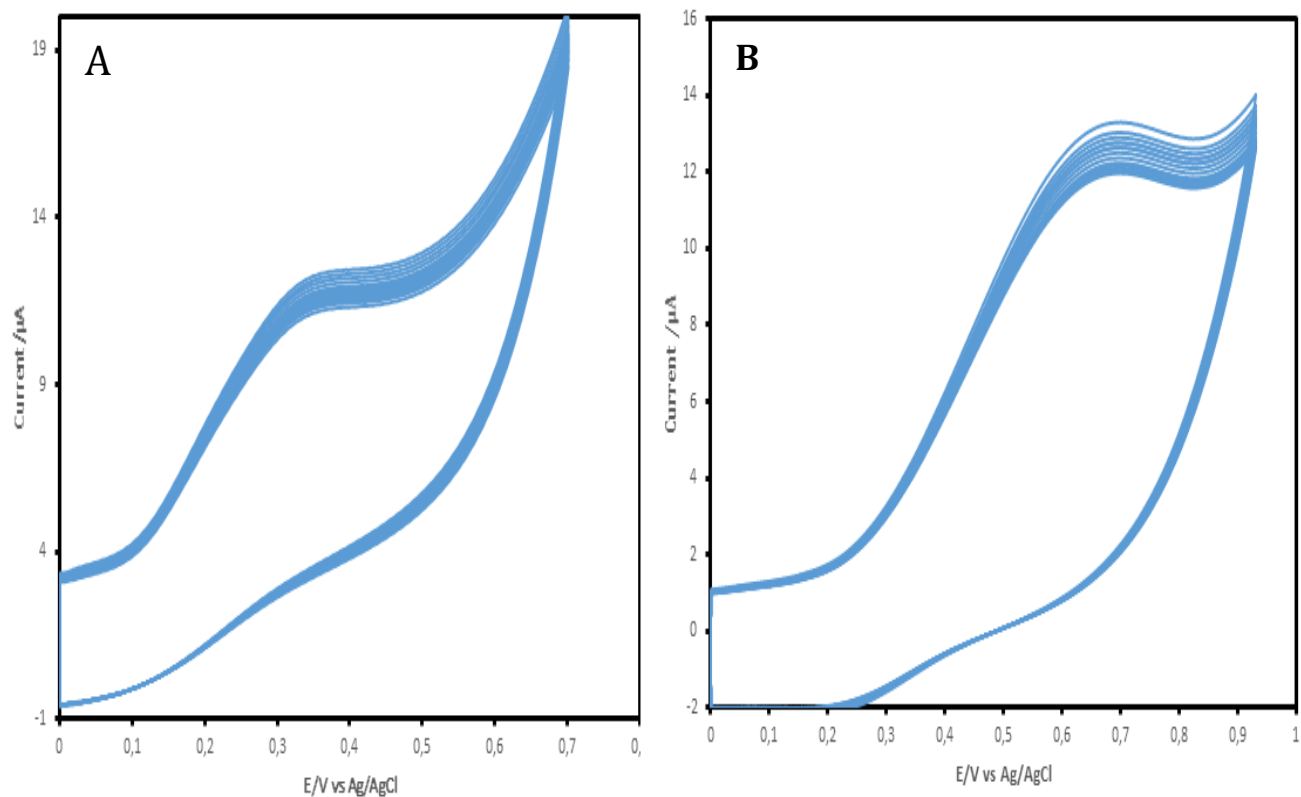
Fig 4.22: A and B shows a 20 cycle continuous scan voltammograms for NGO-NiTAPc-GCE in 1mM Ascorbic acid and Vanillin respectively.

4.18 Stability Studies

The stability of NGO-NiTAPc/GCE under working conditions was investigated by cyclic voltammetry by continuous scanning the electrode for 20 cycles in the presence of equimolar solutions of Ascorbic acid and Vanillin .Fig 4.23 indicates the response stability of NGO-NiTAPc/GCE to equimolar solutions of Ascorbic acid and Vanillin solution at a scan rate of 0.1 V/s and a potential range of 0.1 to 0.9 V .As shown the anodic peak current of both Ascorbic acid and Vanillin oxidation remained almost constant during the experiment indicating that the was no signal loss for the sensor.

Figure 4.23 Continuous cyclic voltammetric evolutions for equimolar solution of ascorbic acid (i) and (ii) vanillin generated on GCE modified with NGO-NiTAPc. Scan rate = 100 mV/s. pH 7 PBS

4.19 Reproducibility

To evaluate the reproducibility of NDGONS-NiTAPc modified GCE for the determination of ascorbic acid and vanillin (Fig 4.24 A and B) respectively ,we take successive measurements of differential pulse voltammetry in 0,1 M PBS pH 7 containing mM Ascorbic acid and Vanillin for 5 times .The modified surface area provided better reproducibility as indicated by the slight decrease in the peak current after washing the electrode and sonicating it in ethanol The

calculated percentage signal loss for the electrode was 2.77 % and 1.83 % respectively, these

values were below 5 % and this indicated good repeatability of the modified electrode .
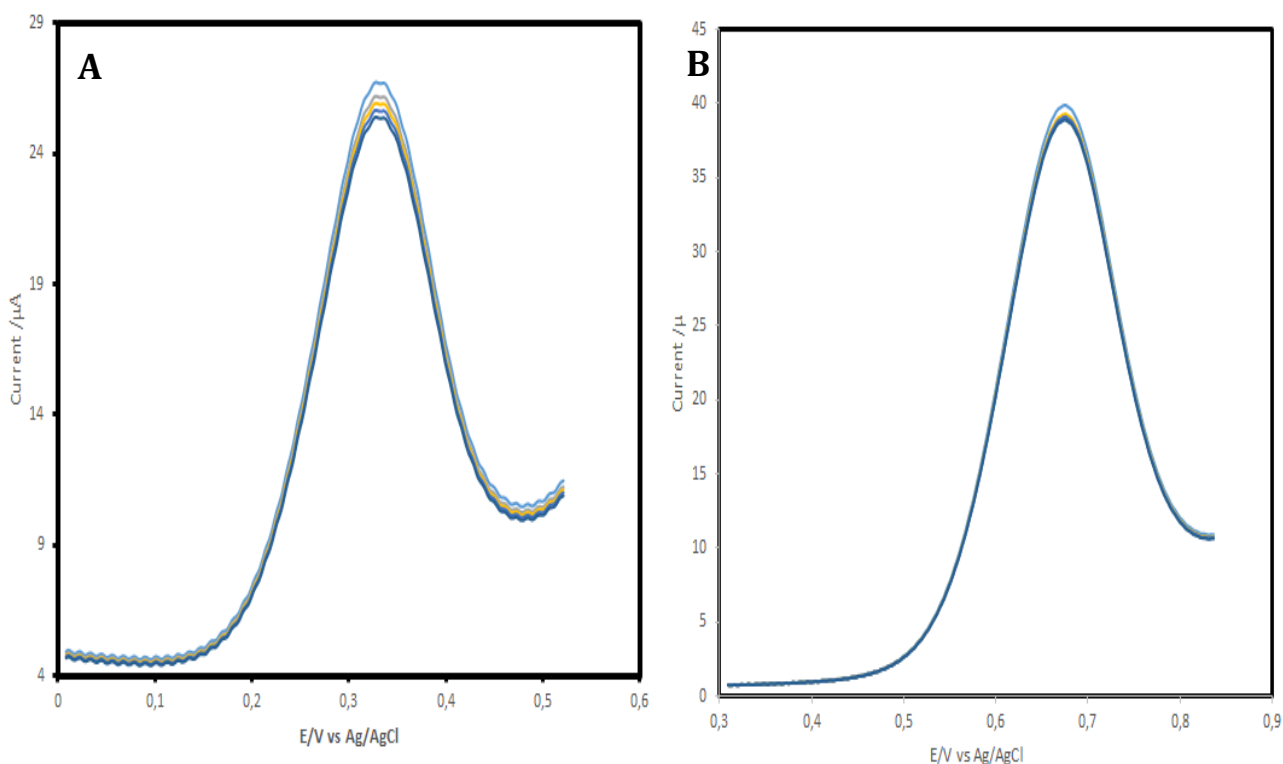
Fig 4.24: Reproducibility of a) ascorbic acid and b) vanillin in 0.1M PBS at pH 7.

4.20: Interference Studies

Equal concentration of vanillin and citric acid ,ascorbic acid and citric acid, vanillin, ascorbic

acid and citric acid were measured and ran separately and voltammogramms were obtained and

recorded. The oxidation peaks of ascorbic acid, vanillin and citric acid was found at 0.3 V, 0.7 V

and 1.15 V respectively. From Fig 4.25 it was deduced that citric acid do not interfere with

vanillin and ascorbic acid during determination. The relative percentage response of the sensor

calculated using the formulae:

$$(R \%) = [1 - (\frac{I^{analyte} + I^{inter}}{I^{inter}})] \times 100 \qquad (4.6)$$

Where $I^{analyte}$ and I^{inter} are the peak currents for both vanillin and ascorbic acid, and for the interfering respectively. The RSD % above 10 % shows that the compound interferes with the analyte . Interferences (citric acid) showed to have no effect as they had interference effect of less than 10 %. The RSD (%) were 6.2% for vanillin and 6.5% ascorbic acid.
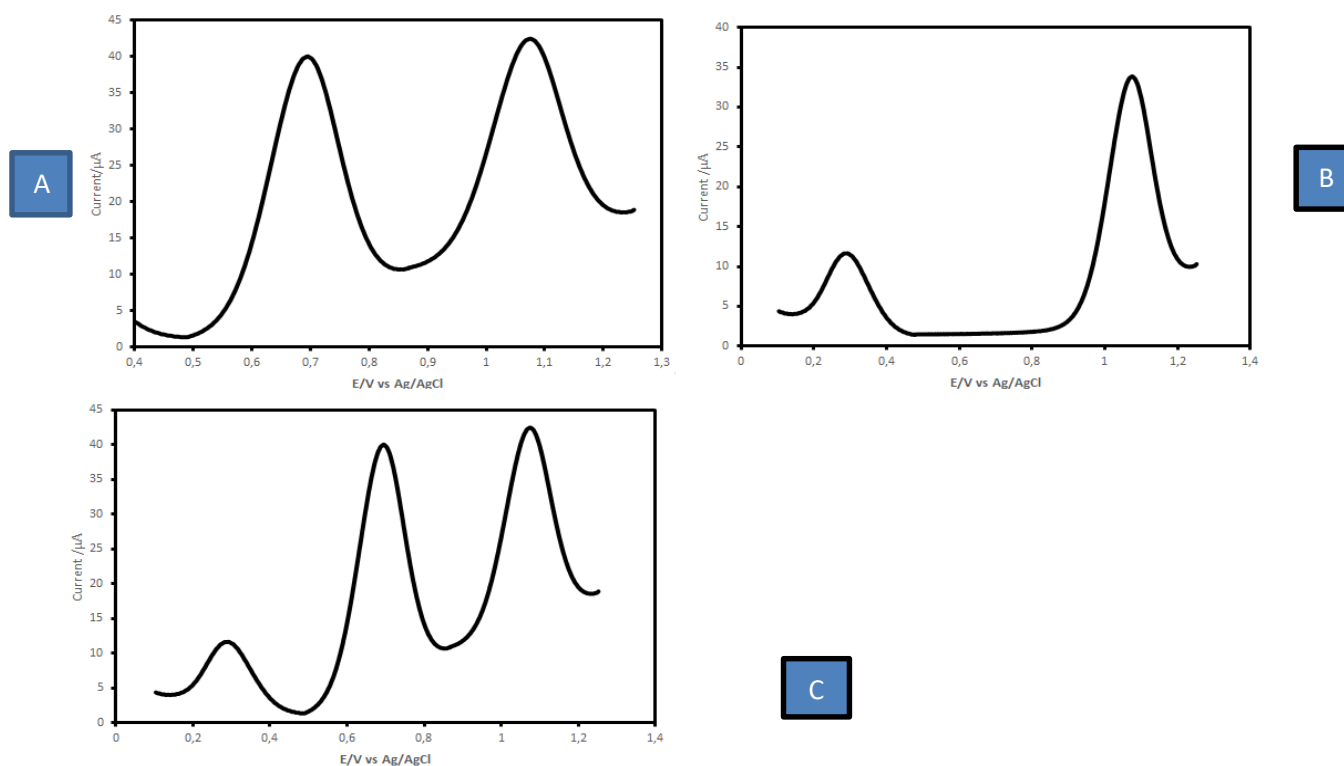
Fig 4.25 : Equimolar concentrations of vanillin and citric acid (a) , ascorbic acid and citric acid (b) , ascorbic acid ,vanillin and citric acid (c).

4.21: Application Studies

4.21.1 Analysis of vanillin in vanilla biscuits

The DPV technique was employed for the standard addition method. In order to estimate the accuracy of the proposed analytical technique, vanilla biscuits was spiked with aliquots amount of vanillin standard. At first the modifier was ran in a blank sample containing only water and a buffer solution of 0.1 M PBS at pH 7, and then solutions of vanillin were added successively for 3 more runs. As can be seen from the figure below, the peak height increases in adding vanillin.
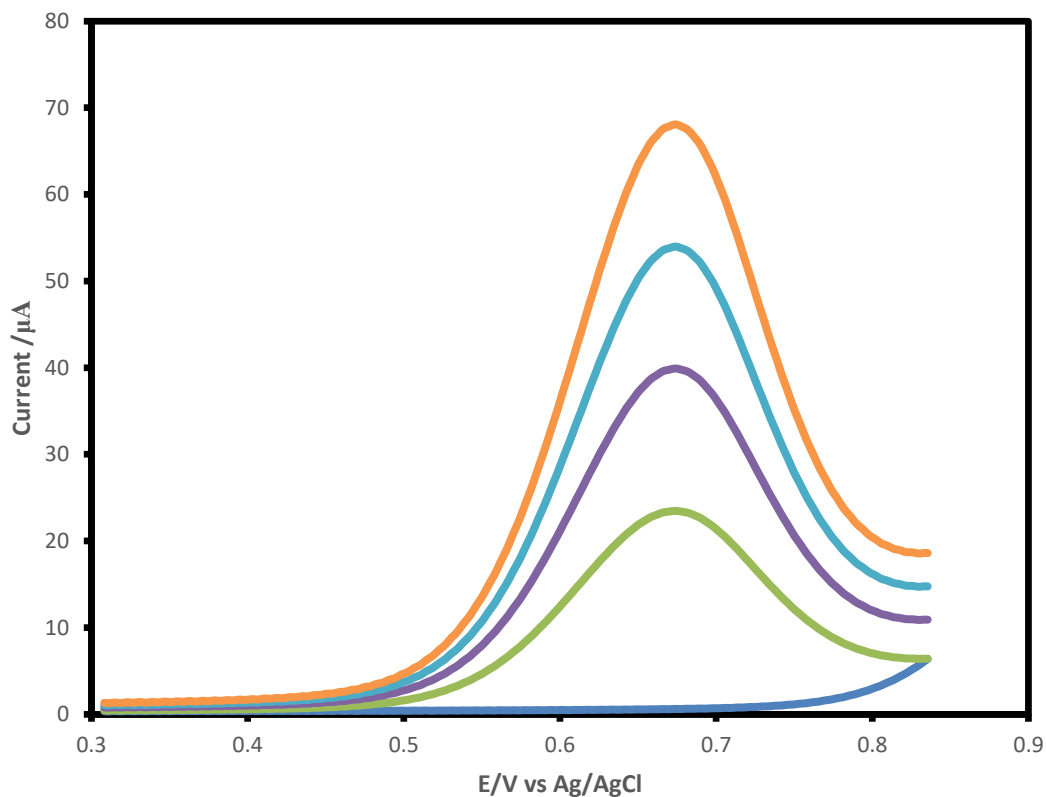
Fig 4.26 DPV voltammograms for real sample analysis for vanillin (a) vanilla biscuits solution+ PBS pH 7 (b) real sample (c) 4 μM (d) 6 μM and (e) 8 μM standard solutions for vanillin.

The average results for five replicate measurements are shown in table 4.5

Table 4.5 shows the average results for five replicate measurements with standard deviation are summarized in table below:

Sample	Added (μm)	Expected (μm)	Found (μm)	(%) Recovery	(%) Recovery In ref [71]
1	0	-	0.75		
2	4	4.75	4.98	106	102
3	6	6.75	6.47	95	96
4	8	8.75	8.72	99	98

4.21.2: Analysis of Ascorbic acid in citrus fruit juice

The DPV technique was employed for the standard addition method. In order to estimate the accuracy of the proposed analytical technique, orange juice was spiked with aliquots amount of ascorbic acid standard. At first the modifier was ran in a blank sample containing only water and a buffer solution of 0.1M PBS at pH 7, and then standard solutions of ascorbic acid were added successively for 3 more runs as shown in Fig 4.27**.**
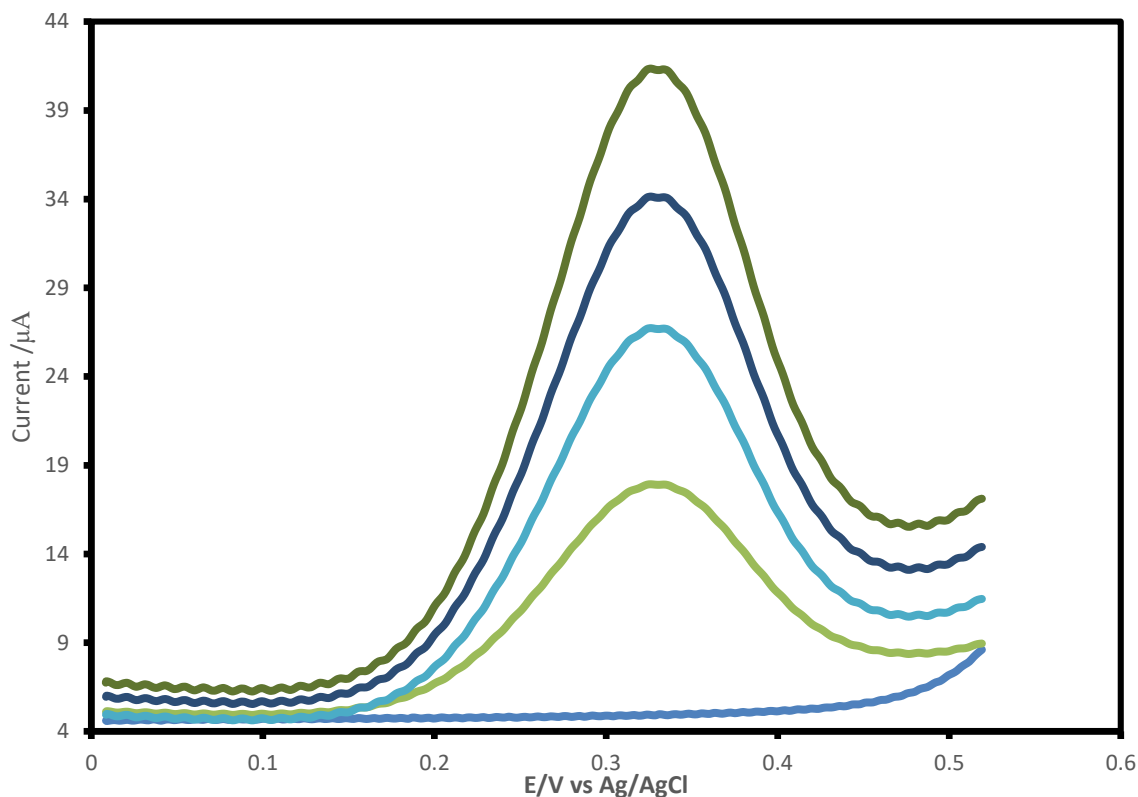
Fig 4.27 DPV voltammograms for real sample analysis for Ascorbic acid (a) orange fruit juice + PBS pH 7 (b) real sample spiked (c) 4 μM (d) 6 μM and (e) 8 μM standard solutions of ascorbic acid.

Table 4.6 shows average results for five replicate measurements with standard deviation are summarized in table below:

Sample	Added (μm)	Expected (μm)	Found (μm)	(%) Recovery	(%) Recovery In Ref [72]
1	0	-	1.3		
2	4	5.3	5.45	102	106

3	6	7.45	7.15	95	98
4	8	9.4	8.99	96	97

CHAPTER 5

CONCLUSION AND RECOMMENDATIONS

5.1 Conclusion

An electrochemical sensor has been developed based on nitrogen doped graphene modified glassy carbon electrode. The use of FTIR was used to monitor the changes in the positions of the $C = O$ vibronic bands as way of confirming chemical linkage within NGO. the IR spectra obtained for the NITAPC, which showed peaks at 3443.00 cm^{-1} assigned for O-H stretching and peak at 1704.01 cm^{-1} is assigned to the C=O. The peaks at 1626 cm^{-1} 1496 cm^{-1} and 1084 cm^{-1}, which coincided with the following bands O – H, C = C, C – C, and C – O respectively. The peak at between 1550 cm^{-1} and 1640 cm^{-1} are assigned to the N-H for the amide group in the metal phthalocyanines.

An electrochemical sensor based on Nickel tetraamine phthalocyanine and nitrogen doped grapheme oxide (NITAPC-NDGONS (mix)) nanoparticles was developed for the simultaneous electrocatalytic oxidation of Vanillin and Ascorbic acid. FTIR, Electrochemical impedance spectroscopy (EIS) and Bode plots were used in the characterization of the synthesized modifiers (NITAPC), (GONS-NITAPC) and NITAPC-NDGONS (mix)). While cyclic voltammetry, linear sweep, chronoamperometry and differential pulse voltammetry were used to assess the electrocatalytic efficiency of the product towards oxidation of Vanillin and ascorbic acid. The surface area of the modified electrode was 0.173 cm^2 and the surface coverage was 7.60 x 10^{-13} mol cm^2. The catalytic rate constant of ascorbic acid was 1.59 x 10^8 M^{-1} s^{-1} and for vanillin it was 1.28 x 10^8 M^{-1} S^{-1} and the apparent electron transfer rate constant was 2.05 x 10^{-2} cm s^{-1} .The adsorption equilibrium constant for ascorbic acid was 6.4 x 10^2 M^{-1} and for vanillin was 8.05 x

10^2 M^{-1} . Gibbs free energy for ascorbic acid was -16.01 kJ and for vanillin was -16.57 kJ. The limit of detection was 8.6 x 10^{-8} M and the limit of quantification was 2.6 x 10^{-7} M for ascorbic acid and LOD was 2.58 x10^{-8} M and LOQ was 6.8 x 10^{-8} M for vanillin. Interference studies were done and the electrode displayed the ability to detect both vanillin and ascorbic acid in the presence of citric acid .The electrode displayed good reproducibility.

5.2 Recommendations

The NDGONS-GCE,GONS-NITAPC-GCE,NDGONS-NITAPC-GCE (mix) electrodes can be used for detection of analytes which are reduced at very high potentials and further studies can still be done in order to enhance the performance of this newly developed modifier. The effectiveness of dopants towards the detection of Vanillin and ascorbic acid can also be investigated by making use of boron or phosphorous doped graphene . In our study we used the dip and dry method for electrode modification. The process involves the modifier solution being dropped onto the electrode surface and then allowed to dry. The disadvantages are that the electrode surfaces are not reproducible and unstable over long periods of time. . Further work can be done using different electrode modification techniques so as to promote reproducibility.

REFERENCES

[1] Ravendra Kumar, P. K. Sharma, Prem Shanker Mishra. A Review on the Vanillin derivatives showing various Biological activities. 2012. 4. 1. 266-279.

[2] Yuxia Liu, Yunzhen Liang, Huan Lian, Cuizong Zhang, Jinyun Peng. Sensitive Voltammetric Determination of Vanillin with an Electrolytic Manganese Dioxide−Graphene Composite Modified Electrode. 2015.10. 4129 – 4137.

[3] Hang Zhu and Guifen Xu. Electrochemical Determination of Ascorbic Acid Based on Hydrothermal Synthesized ZnO Nanoparticles. 2017. 3873 – 3882.

[4] Abdelmajid Sadiki lamari, Anass el fattouh, Salah Eddine el qouatli, Rachida najaih, Abdelilah chtaini. electrochemical detection of ascorbic acid using a polymer modified carbon paste electrode.2013. 39- 42.

[5] Aysun Hacisevkd. An overview of ascorbic acid bio-chemistry. 2009. 38 .3. 233-255

[6] Francesca Capone, Giovanni Colonna, Giuseppe Castello, Susan Costantini, Ascorbic Acid: Its Role in Immune System and Chronic Inflammation Diseases 2014.14. 1-3

[7] Thompson, Garrett, Electrochemical Detection of Antioxidants 2016. Honors Theses and Capstones. 314. http://scholars.unh.edu/honors/314.

[8] Nurulkhalilah Tukimin , Jaafar Abdullah and Yusran Sulaiman , Development of a PrGO-Modified Electrode for Uric Acid Determination in the Presence of Ascorbic Acid by an Electrochemical Technique.2017.17.1-12.

[9] Adriana Covarrubias-Pinto, Aníbal Ignacio Acuña, Felipe Andrés Beltrán, Leandro Torres-Díaz and Maite Aintzane Castro. Old Things New View: Ascorbic Acid Protects the Brain in Neurodegenerative Disorders.2015.16. 28194–28217

[10] Suhera M Aburawi, Fathia AGhambirlou, Asseid A Attumi, Rida A Altubuly1 and Ahmed A Kara, Effect of Ascorbic Acid on Mental Depression Drug Therapy: Clinical Study.2014.4.1.

[11] Levine M, Rumsey SC, Dhariwal KR, Park J & Wang Y. Criteria and recommendation for ascorbic acid intake. J Amer Med Assoc 1999.281.1415-1423.

[12]Mark Levine, Yaohui Wang, Sebastian J. Padayatty, and Jason Morrow, A new recommended dietary allowance of vitamin C for healthy young women. 2001 .98.17. 9842–9846.

[13] Neuhauser, E.F. et al, Soil invertebrates and the degradation of Vanillin, cinnamic acid and lignins. Soil Biol. Biochem.2009. 10. 5.431- 435.

[14] Jinyun Peng, Chuantao Hou , Xiaoya Hu1, A graphene-based electrochemical sensor for Sensitive Detection of Vanillin, Int. J. Electrochem. Sci. 2012 .7.1724 – 1733.

[15] Yao Y, Bai X, Shiu K. Carbon Nanotubes and the Application .2012.428–44.

[16] Allen J. Bard, Chemical Modification of Electrodes.1983.13.135-145

[17] Schreurs, J. P. G. M. Surface modified electrodes: an exploration into preparation, characterization and possibilities.2004. DOI: 10.6100/IR148276

[18] Colby A.Foss, Jr and C.R.martin, chemically modified electrodes. journal of physical chemistry.1994.77.1401-1406

[19] Aoife Morrin, Development in modified electrodes for sensing applications.2004.1-239

[20] Carolina Maria Fioramonti Calixtoa, Renata Kelly Mendes, Aline Carlos de Oliveira, Development of Graphite-Polymer Composites as Electrode Materials.2007.10. 2. 109-114.

[21] Samuel P. Kounaves, Voltammetric Techniques.2001.709-725.

[22] Stephen K. Lower, Electrochemistry.2004

[23] Adrian W. Bott, Mass Transport.1994. 14.3.103-108

[24] A.Salimi, H.M.Khezri, R.Hallaj, Talanta. Introduction and Overview of Cyclic Voltammetry and Its Theoretical Considerations. 2006. 70.823-835

[25] J.P.Renault, A.Bemard, A.Bietsch, B.Michel, H.R.Bosshard, E.B.Dalamarche, M.Kleiter, B.Hecht, U.P.Wild, J.Phys.Chem.B. 2003.70.703-712

[26] R.Parsons, Surf. Sou, 1990.90. 813.

[27] J.J.V.Benschoten, J.Y.Lewis, W.R.Heineman, D.A.Roston, P.T.Kissinger, J. Chem. Educ, 60.19.772-778.

[28] John .C and Michael .T The Theory experiment and application voltammetric techniques 2009:134‑82014.6.7525‑31.

[31] Siswana MP, Ozoemena KI, Geraldo DA, Nyokong T. Nanostructured nickel (II) phthalocyanine — MWCNTs as viable nanocomposite platform for electrocatalytic detection of asulam pesticide at neutral pH conditions 2010:1351–8. doi:10.1007/s10008-009-0958-3.

[32] Zhao Y, Du Y, Lu D, Wang L, Ma D. Analytical Methods Sensitive determination of vanillin based on an arginine functionalized graphene fi lm 2014:1753–8. doi:10.1039/c3ay41517a.

[33] Mugadza T, Nyokong T. Electrochimica Acta Synthesis and characterization of electrocatalytic conjugates of tetraamino cobalt (II) phthalocyanine and single wall carbon nanotubes 2009;54:6347–53. doi:10.1016/j.electacta.2009.05.074.

[34] Maringa A, Mugadza T, Antunes E, Nyokong T. Author personal copy Characterization and electrocatalytic behaviour of glassy carbon electrode modified with nickel nanoparticles towards amitrole detection . 2009.54: 6347–53. doi:10.1016/j.electacta.2009.05.074

[35] Shumba M, Nyokong T. Electrode modification using nanocomposites of boron or nitrogen doped graphene oxide and cobalt (II) tetra aminophenoxy phthalocyanine nanoparticles. Electrochim Acta 2016.196:457–69. doi:10.1016/j.electacta.2016.02.166.

[36] Huang L, Hou K, Jia X, Pan H, Du M. Preparation of novel silver nanoplates / graphene composite and their application in vanillin electrochemical detection. Mater Sci Eng C 2014;38:39–45. doi:10.1016/j.msec.2014.01.037.

[37] Chen C, Shi M, Xue M, Hu Y. Synthesis of nickel (II) coordination polymers and conversion into porous NiO nanorods with excellent electrocatalytic performance for glucose detection †. RSC Adv 2017;7:22208–14. doi:10.1039/C7RA00715A.

[38] Faisal SN, Haque E, Noorbehesht N, Zhang W, Harris AT, Church TL, et al. RSC Advances. RSC Adv 2017;7:17950–8. doi:10.1039/C7RA01355H.

[39] Online VA, Yan Z, Wu Y, Di J. RSC Advances 2014. doi:10.1039/C4RA13653E.

[40] Eun-Young Cho, Tae Hee Han, Jihyun Hong, Ji Eun Kim, Sun Hwa Lee, Hyun, Noncolvalent Functionalization of Graphene with End-Functional Polymers.2010 .

[41] Satish Bykkam, Venkateswara Rao K, Shilpa Chakra C.H and Tejaswi Thunugunta, synthesis and characterization of graphene oxide and its microbial activity against staphylococcus.2013. 4. 1. 142-146.

[42] Burcu Dogan-Topal, Sibel A. Ozkan and Bengi Uslu , The Analytical Applications of Square Wave Voltammetry on Pharmaceutical Analysis. The Open Chemical and Biomedical Methods Journal. 2010. 3.56-73

[43] Krause, J., Matthew, S., Ramaley, L., "Analytical Application of Square Wave Voltammetry", Anal. Chem.1969.41.11 .1365-8

[44] Shirley Theodora Rose Le Roux, The application of differential pulse stripping voltammetry in the determination of trace metals in wet precipitation.1999.

[45] Samuel P. Kounaves. Voltammetric Techniques.2001.709-725.

[49] Cook M.J., Chambrier I., Cracknell S.J., Mayes D.A., Russell D.A. Octa-alkyl zinc phthalocyanines: Potential photosensitizers for use in the photodynamic therapy of cancer. Phtotochemistry and Phthobiology.1995. 62. 542-545

[50] Dougherty T.J. Photodynamic Therapy. Phtotochemistry and Phthobiology.1993. 58. 895-9

[51] Moan J. Properties for optimal PDT sensitizers, Journal of Photochemistry and Photobiology B: Biology.2007. 5.521-524.

[52]   Maringa A, Mugadza T, Antunes E, Nyokong T. Characterization and electrocatalytic behaviour of glassy carbon electrode modified with nickel nanoparticles towards amitrole

detection. J Electroanal Chem 2013;700:86–92. doi:10.1016/j.jelechem.2013.04.022.

[53]   Manuscript A. rsc.li/njc 2017. doi:10.1039/C7NJ01857F.

[54]   Nyoni S, Mugadza T, Nyokong T. Improved l-cysteine electrocatalysis through a sequential drop dry technique using multi-walled carbon nanotubes and cobalt tetraaminophthalocyanine conjugates. Electrochim Acta 2013. doi:10.1016/j.electacta.2013.10.023.

[55]   Amidi S, Ardakani YH, Ranjbari E, Sepehri Z, Bagheri H. Sensitive electrochemical determination of rifampicin using gold nanoparticles/poly-melamine nanocomposite. RSC Adv 2017;7:40111–8. doi:10.1039/C7RA04865C.

[56]   Raj CR, Ohsaka T. Electrocatalytic sensing of NADH at an in situ functionalized self-assembled monolayer on gold electrode 2001;3:633–8.

[57]   Barman K, Jasimuddin S. RSC Advances. RSC Adv 2016;6:20800–6. doi:10.1039/C5RA26534G.

[58]   Mugadza T, Nyokong T. Author â€™ s personal copy Covalent linking of ethylene amine functionalized single-walled carbon nanotubes to cobalt (II) tetracarboxyl-phthalocyanines for use in electrocatalysis n.d. doi:10.1016/j.synthmet.2010.07.036.

[59]   Mamuru SA, Ozoemena I. Heterogeneous Electron Transfer and Oxygen Reduction Reaction at Nanostructured Iron (II) Phthalocyanine and Its MWCNTs Nanocomposites 2010:985–94. doi:10.1002/elan.200900438.

[60]   Xiong W, Wu M, Zhou L, Liu S. RSC Advances The highly sensitive electrocatalytic sensing of catechol using a gold / titanium dioxide. RSC Adv 2014;4:32092–9.

doi:10.1039/C4RA04256E.

[61]   Manuscript A. rsc.li/pccp 2016. doi:10.1039/C6CP08360A.

[62]   Mugadza T, Arslano Y. Author â€™ s personal copy Electrochimica Acta (II)— Single walled carbon nanotube conjugate platforms and their use in electrocatalysis of amitrole n.d. doi:10.1016/j.electacta.2012.02.041.

[63]   Peng J, Feng Y, Han X, Gao Z. Simultaneous determination of bisphenol A and hydroquinone using a poly (melamine) coated graphene doped carbon paste electrode. Microchim Acta 2016. doi:10.1007/s00604-016-1865-9.

[64]   Sivakumar M, Sakthivel M, Chen S. Simple synthesis of cobalt sulfide nanorods for efficient electrocatalytic oxidation of vanillin in food samples. J Colloid Interface Sci 2016. doi:10.1016/j.jcis.2016.11.094.

[65] Narasimharao K, Venkata Ramana G, Sreedhar D, Vasudevarao V (2016) Synthesis of Graphene Oxide by Modified Hummers Method and Hydrothermal Synthesis of Graphene-NiO Nano Composite for Supercapacitor Application. J Material Sci Eng 5: 284. doi:10.4172/2169-0022.1000284.

[66] Ntsendwana B, Mamba BB, Sampath S, Arotiba OA. Electrochemical Detection of Bisphenol A Using Graphene- Modified Glassy Carbon Electrode 2012;7:3501–12.

[67] Mugadza .T.Tebello Nyokongo . Synthesis and electrocatalytic behavior of cobalt (II)-tris(benzyl-mercapto)-monoaminophthalocyanine–single walled carbon nanotube nanorods. Electrochimica Acta .2010.

[69]Abraha Tadese, P. A. Subramanian, Amaha Woldu and Rishi Pa. Electrochemical determination and comparison of ascorbic acid in freshly prepared and bottled fruit juices: A cyclic voltammetric study. Journal of Chemical and Pharmaceutical Research. 2014. 6.5.880-888

[70] Yavuz Yardım, Mehmet Gulcan , Zuhre Senturk. Determination of vanillin in commercial food product by adsorptive stripping voltammetry using a boron-doped diamond electrode. Food Chemistry. 2013.141. 1821‑1827